Los Alamos
NATIONAL LABORATORY

UNIVERSITY of VIRGINIA

Possibilities with Polarized Targets

D. Keller
UVA

SOLID POLARIZED TARGET GROUP at the UNIVERSITY of VIRGINIA

Outline

- Understanding Internal Structure
- Introduction to The Target
- Spin-1 Solid Polarized Target
- High Intensity Photon Source
- Conclusion

Understanding Dynamics

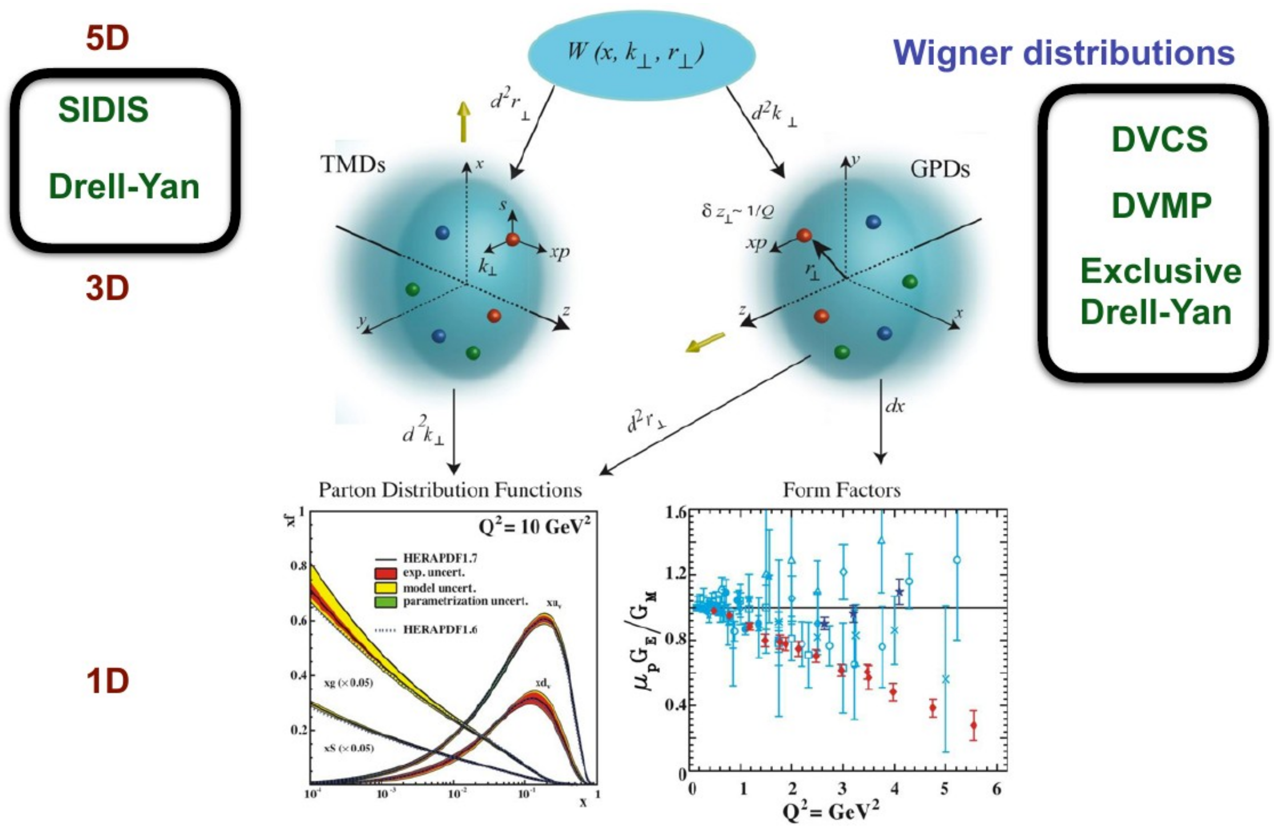

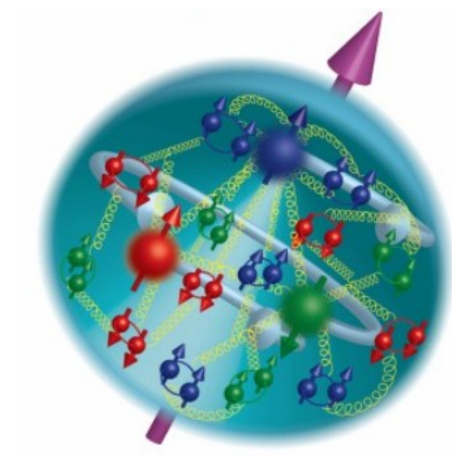

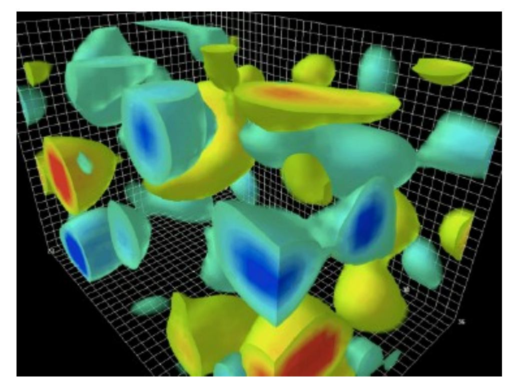

- Need Additional Tools
- Need Complete Framework

What is a Solid Polarized Target

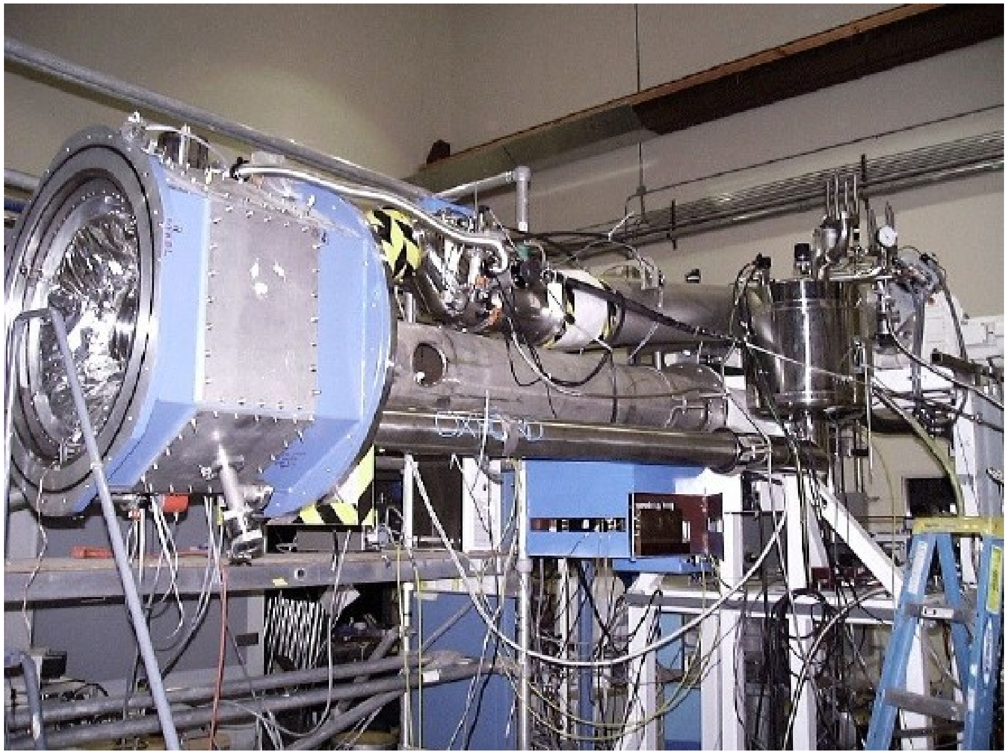

- A marriage of sciences for the purpose of optimizing the over all figure of merit of Nuclear/Particle Spin Physics
- Use of high density, high polarizability, with high interaction rate in fixed target experiments

Dynamic Nuclear Polarization

Add Free Radicals, cool sample, RF-sample in B-field

e⁻ relaxation ~ms

P relaxation ~10s of min.

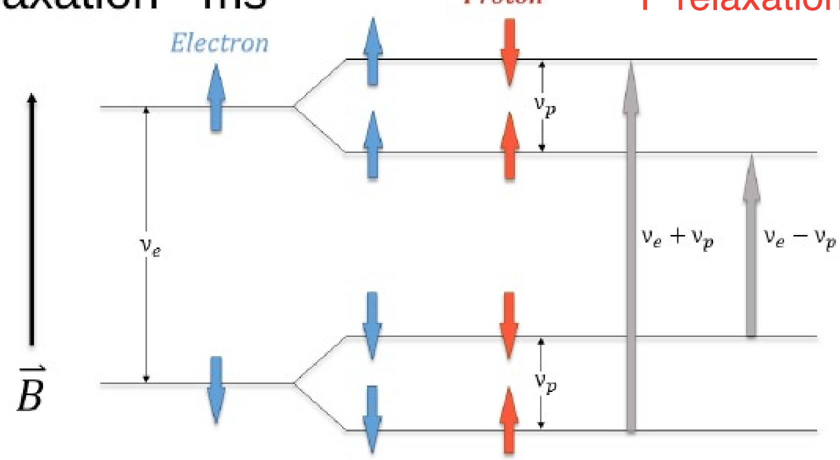

Zeeman Splitting

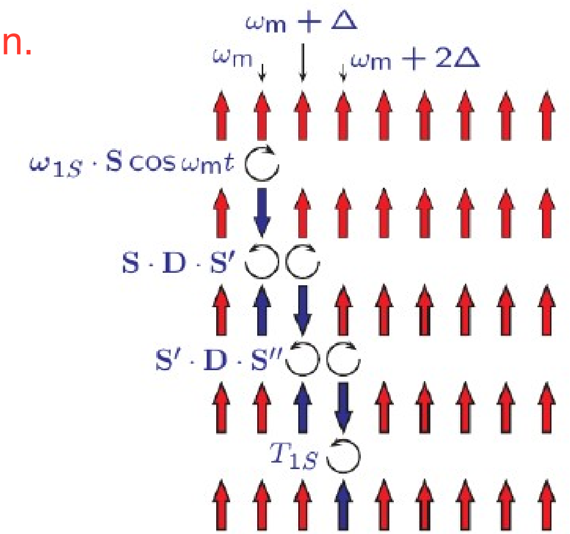

flip-flop rate $\frac{1}{T_{2S}}$

diffusion rate $\frac{1}{\omega_{0I} T_{2S}^2}$

5T: 140 GHz

2.5: 70 GHz

- narrow ESR line $< \omega_{0I}$ — well-resolved solid effect
- broad ESR line $> \omega_{0I}$
  - weak μ-wave field $\omega_{1S} T_{2S} < 1$
    - fast spectral diffusion $\frac{1}{\omega_{0I} T_{2S}^2} > \frac{1}{T_{1S}}$ — thermal mixing
    - slow spectral diffusion $\frac{1}{\omega_{0I} T_{2S}^2} < \frac{1}{T_{1S}}$ — cross effect
  - strong μ-field $\omega_{1S} T_{2S} > 1$ — differential solid effect

- Transfer of spin polarization from electrons to nuclei
- Electrons 1K 2.5T ~92%

  Protons 1K 2.5T ~0.25%
- Narrow ESR width will help optimize

Calibrate P:Area

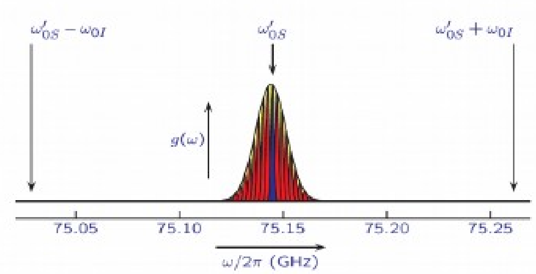

$$P = \frac{e^{\frac{\mu B}{kT}} - e^{\frac{-\mu B}{kT}}}{e^{\frac{\mu B}{kT}} + e^{\frac{-\mu B}{kT}}} = \tanh\left(\frac{\mu B}{kT}\right)$$

Spin Polarization

Spin-1/2 system in B-field leads to 2 sublevels due to Zeeman interaction

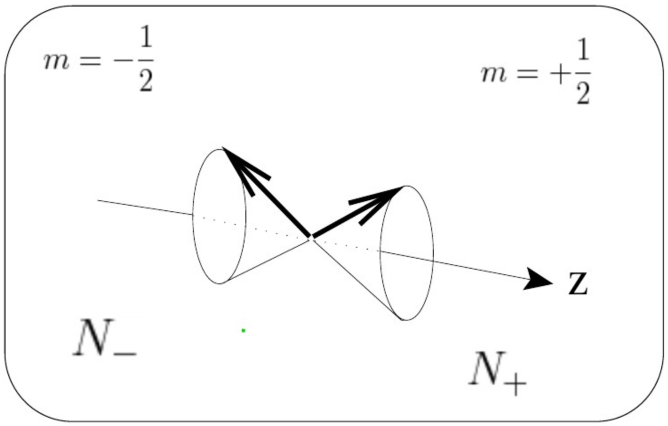

$$P_z = \frac{N_+ - N_-}{N_+ + N_-}$$

-1 < P_z < +1

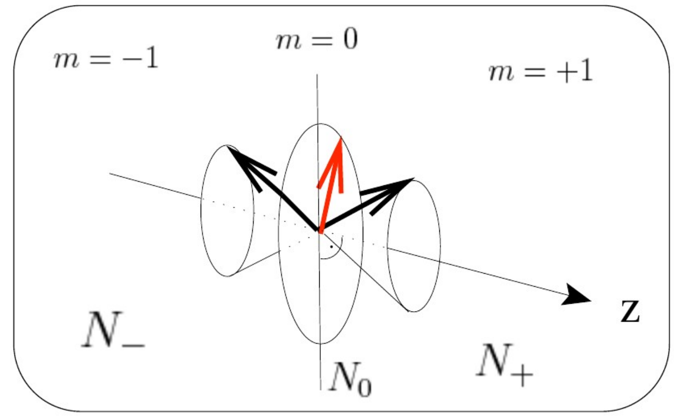

$$P_z = \frac{N_+ - N_-}{N_+ + N_-}$$

$$P_{zz} = \frac{(N_+ - N_0) - (N_0 - N_-)}{N_+ + N_0 + N_-} = \frac{(N_+ + N_-) - 2N_0}{N_+ + N_0 + N_-}$$

Defining Polarization

Spin-1

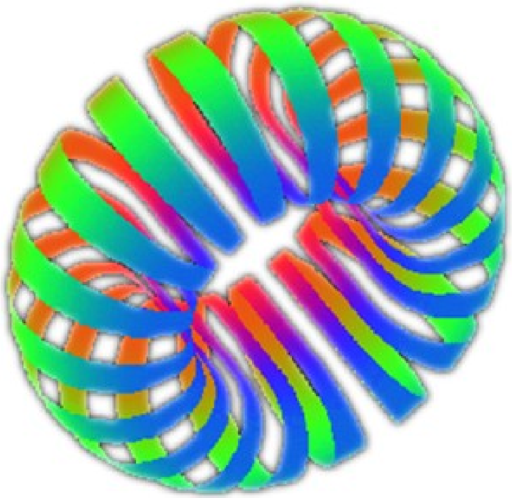

$P_{zz} = -2$

Pure Tensor Polarization

All spins in the m=0 level

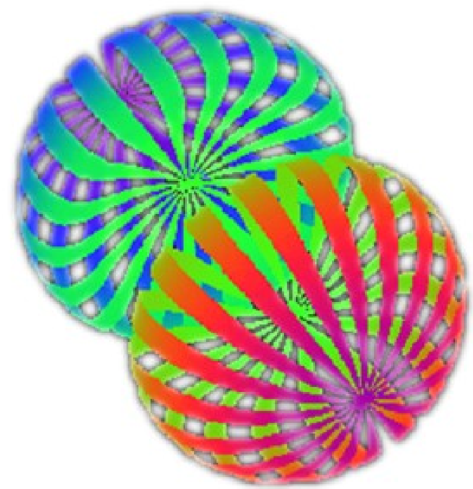

$P_{zz} = +1$

Pure Vector Polarization

m=0 level depopulated

Two nucleon density distributions connected to electromagnetic form factor for spin-1

$-2 < P_{zz} < +1$

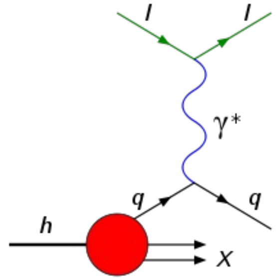

Polarized DIS

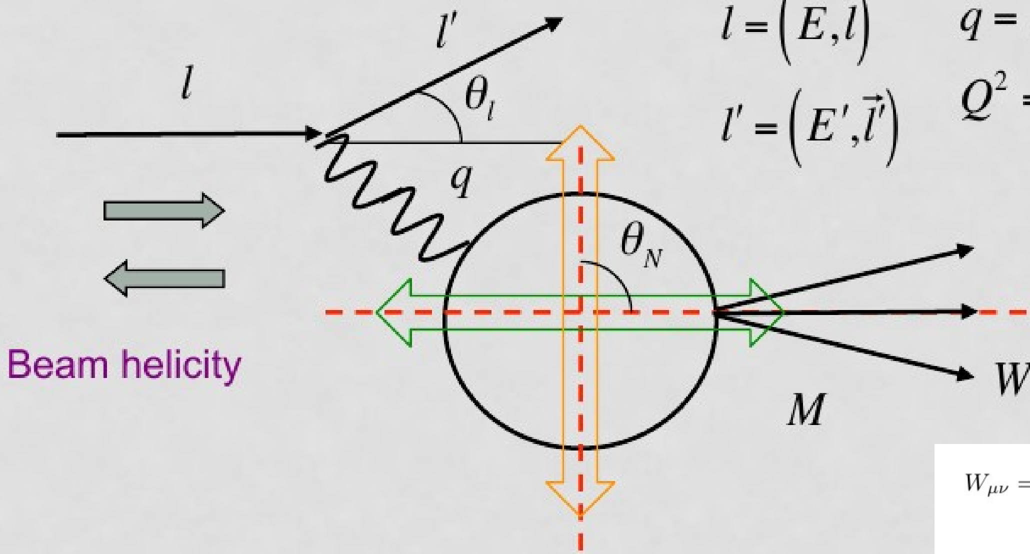

$l = (E, \vec{l})$

$l' = (E', \vec{l}')$

$q = l - l'$

$Q^2 = \vec{q}^{\,2} - \nu^2 = 2EE'(1 - \cos(\theta_{l'}))$

$x = \frac{Q^2}{2M\nu}$

$\nu = E - E'$

$y = \frac{\nu}{E}$

$W^2 = M^2 + 2M\nu - Q^2$

Longitudinal Target Polarization $\theta_N = 0$

Transverse Target Polarization $\theta_N = \pi/2$

$$W_{\mu\nu} = \left(-g_{\mu\nu} + \frac{q_\mu q_\nu}{q^2}\right) F_1(x,Q^2) + \frac{\hat{p}_\mu \hat{p}_\nu}{p\cdot q} F_2(x,Q^2) + i\epsilon_{\mu\nu\alpha\beta}\frac{q^\alpha p^\beta}{2p\cdot q} F_3(x,Q^2)$$
$$- i\epsilon_{\mu\nu\alpha\beta}\frac{q^\alpha s^\beta}{p\cdot q} g_1(x,Q^2) - i\epsilon_{\mu\nu\alpha\beta}\frac{q^\alpha\,(p\cdot q\, s^\beta - s\cdot q\, p^\beta)}{(p\cdot q)^2} g_2(x,Q^2)$$
$$+ \frac{1}{p\cdot q}\left[\frac{1}{2}(\hat{p}_\mu \hat{s}_\nu + \hat{p}_\nu \hat{s}_\mu) - \frac{s\cdot q}{p\cdot q}\hat{p}_\mu \hat{p}_\nu\right] g_3(x,Q^2)$$
$$+ \frac{s\cdot q}{p\cdot q}\left[\frac{\hat{p}_\mu \hat{p}_\nu}{p\cdot q} g_4(x,Q^2) + \left(-g_{\mu\nu} + \frac{q_\mu q_\nu}{q^2}\right) g_5(x,Q^2)\right],$$

Asymmetries in the scattering of polarized leptons on polarized nucleons most sensitive to spin structure functions g_1 and g_2

$$\frac{d^2\sigma^{\uparrow\Uparrow(\Downarrow)}}{d\Omega dE'} = \frac{d^2\sigma}{d\Omega dE'} - (+)\frac{2\alpha^2 E'}{Q^2 E}\left(\frac{E + E'\cos\theta}{M\nu} g_1(x,Q^2) - \frac{Q^2}{M\nu^2} g_2(x,Q^2)\right)$$

Novel Targets for Novel Physics

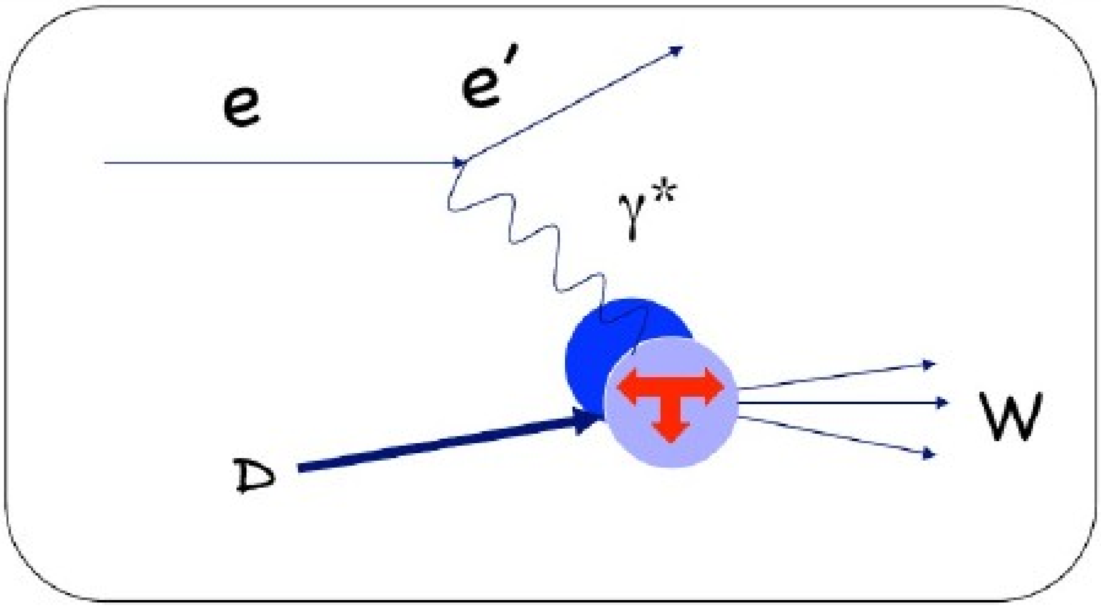

Construct the most general Tensor W consistent with Lorentz and gauge invariance

Frankfurt & Strikman (1983)

Hoodbhoy, Jaffe, Manohar (1989)

	Nucleon	Deuteron
F_1	$\frac{1}{2}\sum_q e_q^2 [q_\uparrow^{\frac{1}{2}} + q_\uparrow^{-\frac{1}{2}}]$	$\frac{1}{3}\sum_q e_q^2 [q_\uparrow^1 + q_\uparrow^{-1} + q_\uparrow^0]$
g_1	$\frac{1}{2}\sum_q e_q^2 [q_\uparrow^{\frac{1}{2}} - q_\downarrow^{\frac{1}{2}}]$	$\frac{1}{2}\sum_q e_q^2 [q_\uparrow^1 - q_\downarrow^1]$
b_1	$--$	$\frac{1}{2}\sum_q e_q^2 \left[2q_\uparrow^0 - (q_\uparrow^1 + q_\uparrow^{-1})\right]$

$$W_{\mu\nu} = -F_1 g_{\mu\nu} + F_2 \frac{P_\mu P\nu}{\nu} + i\frac{g_1}{\nu}\epsilon_{\mu\nu\lambda\sigma} q^\lambda s^\sigma + i\frac{g_2}{\nu^2}\epsilon_{\mu\nu\lambda\sigma} q^\lambda (p \cdot q s^\sigma - s \cdot q p^\sigma)$$

$$-b_1 r_{\mu\nu} + \frac{1}{6} b_2 (s_{\mu\nu} + t_{\mu\nu} + u_{\mu\nu}) + \frac{1}{2} b_3 (s_{\mu\nu} - u_{\mu\nu}) + \frac{1}{2} b_4 (s_{\mu\nu} - t_{\mu\nu})$$

} Tensor Polarization

Probing Polarization of Partons

Resulting in the spin structure observed in the nuclear spin

q^0 : Probability to scatter from a quark (any flavor) carrying momentum fraction x while the *Deuteron* is in state $m=0$

q^1 : Probability to scatter from a quark (any flavor) carrying momentum fraction x while the *Deuteron* is in state $|m| = 1$

Probes a particular aspect of spin-1 internal structure

$$b_1(x) = \frac{q^0(x) - q^1(x)}{2}$$

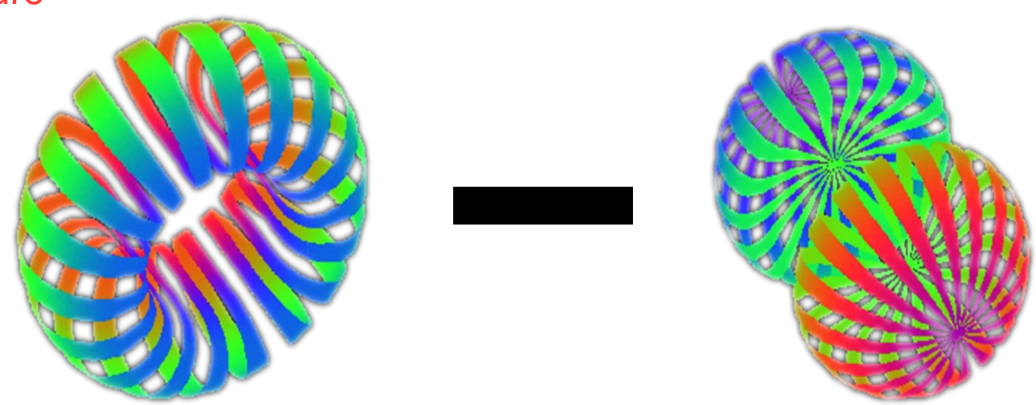

Should be zero for internal constituents being in s-wave

Tensor-Polarized Structure

Magnetic Moment(D) $\approx$ Magnetic Moment(p)+Magnetic Moment(n)

S wave: $\delta_T q_i(x,Q^2) = q_i^0 - \frac{q_i^1 + q_i^{-1}}{2} = 0,\ b_1 = \frac{1}{2}\sum_i e_i^2 (\delta_T q_i(x,Q^2) + \delta_T \bar{q}_i(x,Q^2)) = 0$

S-D Mix: $\delta_T q_i(x,Q^2) = q_i^0 - \frac{q_i^1 + q_i^{-1}}{2} \neq 0,\ b_1 = \frac{1}{2}\sum_i e_i^2 (\delta_T q_i(x,Q^2) + \delta_T \bar{q}_i(x,Q^2)) \neq 0$

where q^m is patron distribution function in hadron spin-m state.

Extraction of Observable

$$A_{zz} = \frac{2}{fP_{zz}} \frac{\sigma_{\dagger} - \sigma_0}{\sigma_0}$$

$$= \frac{2}{fP_{zz}} \left(\frac{N_{\dagger}}{N_0} - 1 \right)$$

Use negative or unpolarized

$$T = \frac{N_T}{R_T} = \frac{16}{P_{zz}^2 f^2 \delta A_{zz}^2 R_T}$$

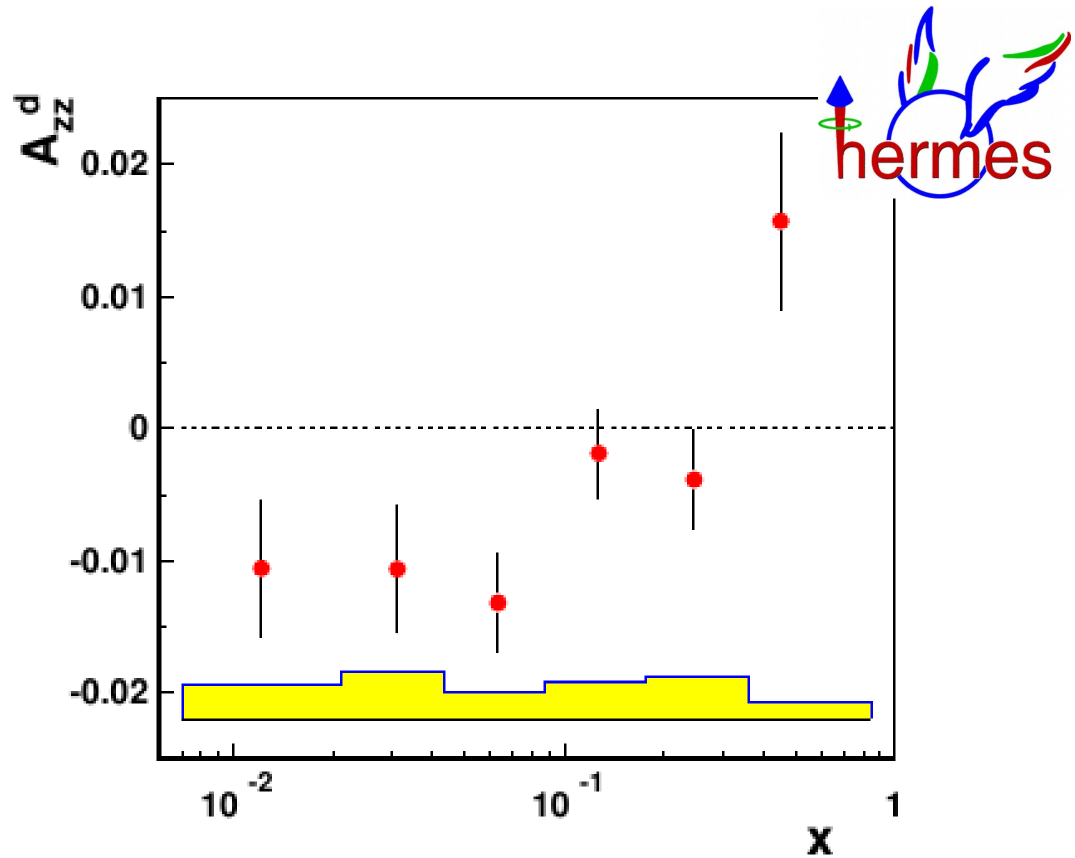

Atomic-gas target

$\sigma_{\dagger}$: Tensor Polarized cross-section

σ_0 : Unpolarized cross-section

P_{zz} : Tensor Polarization

	Hermes	JLAB
P_{zz}	0.8	0.2
Dilution	0.9	0.30
$L(cm^{-2}s^{-1})$	10^{31}	10^{35}

$$b_1 = -\frac{3}{2} F_1^d A_{zz}$$

Extraction of Observable

Hermes data show that b_1 is not as small as the prediction for the S-D mixture proposal

Analysis of the hermes data indicates finite tensor-polarization of the antiquarks at x<0.1

$xb_1 \sim 10^{-4}$

↕ Order of magnitude difference

$xb_1 \sim 10^{-3}$ **in HERMES data**

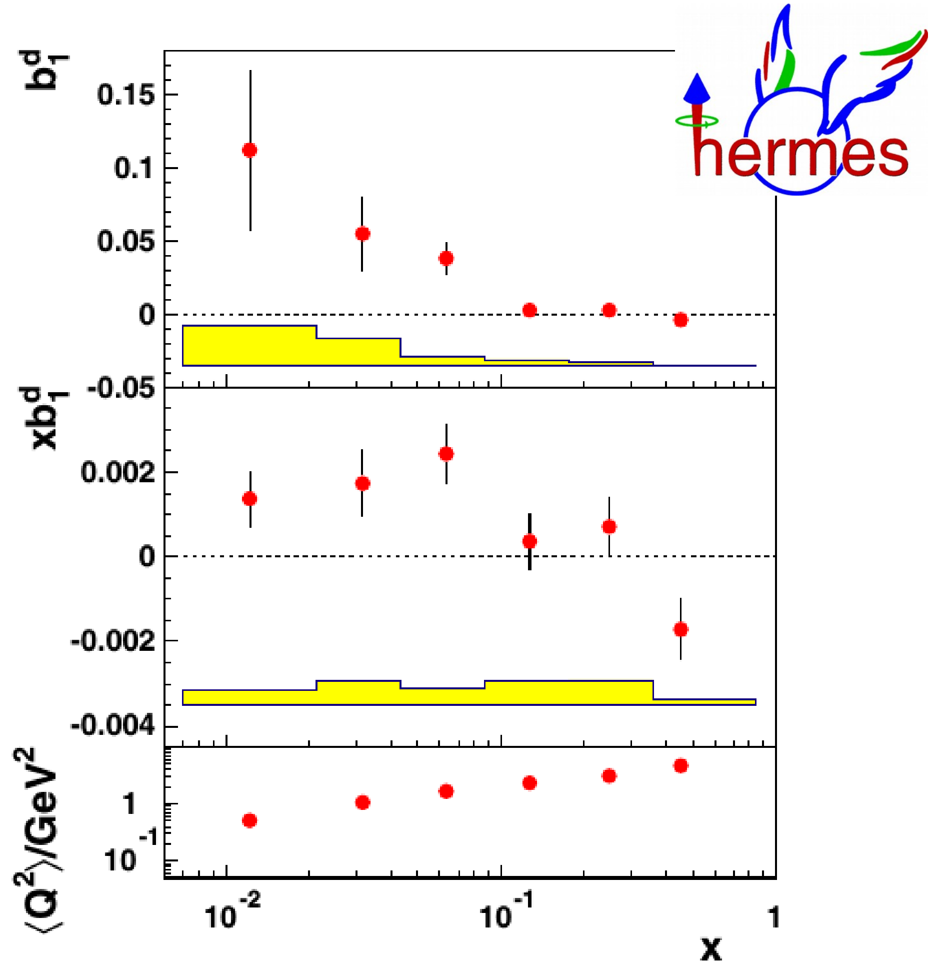

Close-Kumano sum rule relates b1 to the spin-1 elastic form factor the integral of x should be about 10E-4

$$\int_{0.002}^{0.85} b_1(x)dx = [1.05 \pm 0.34(stat) \pm 0.35(sys)] \times 10^{-2}$$

$$\int_{0.02}^{0.85} b_1(x)dx = [0.35 \pm 0.10(stat) \pm 0.18(sys)] \times 10^{-2}$$

Sign change expected for D-state

$$b_1 = -\frac{3}{2} F_1^d A_{zz}$$

Extraction of Observable

$$A_{zz} = \frac{2}{fP_{zz}} \frac{\sigma_{\dagger} - \sigma_0}{\sigma_0}$$

$$= \frac{2}{fP_{zz}} \left(\frac{N_{\dagger}}{N_0} - 1 \right)$$

$$T = \frac{N_T}{R_T} = \frac{16}{P_{zz}^2 f^2 \delta A_{zz}^2 R_T}$$

$\sigma_{\dagger}$: Tensor Polarized cross-section

σ_0 : Unpolarized cross-section

P_{zz} : Tensor Polarization

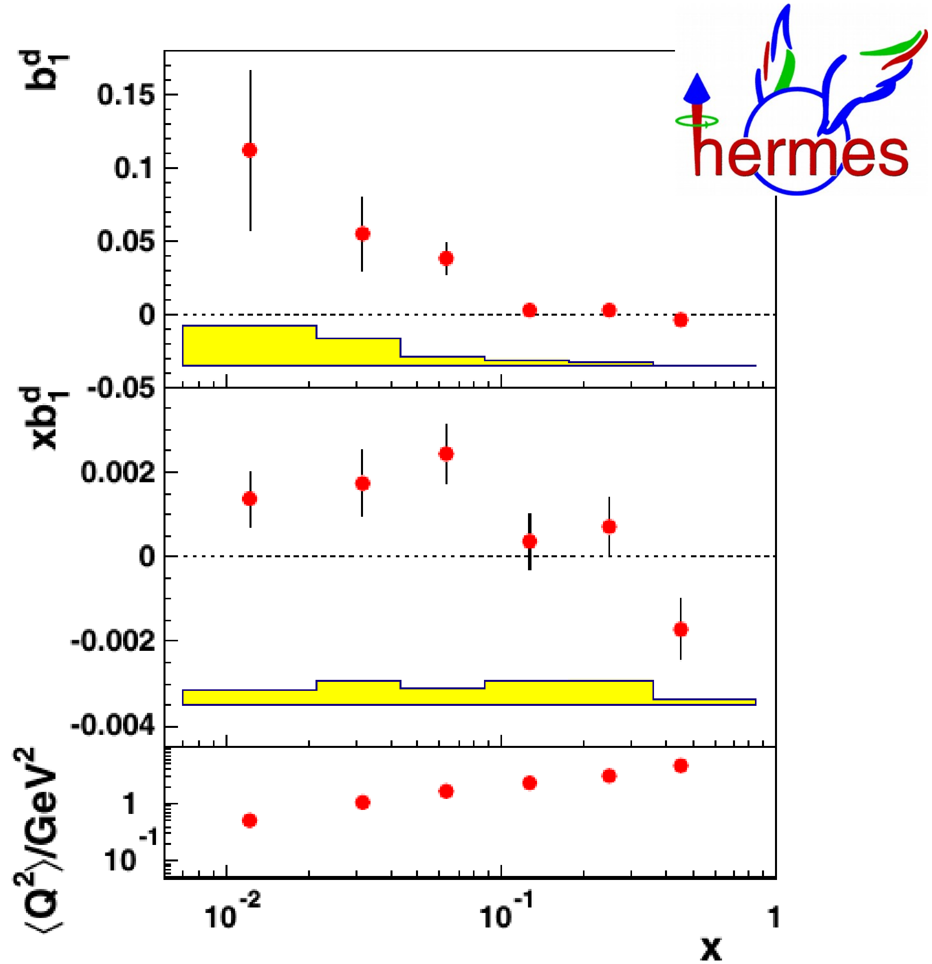

Atomic-gas target

	Hermes	JLAB
P_{zz}	0.8	0.2
Dilution	0.9	0.30
$L(cm^{-2}s^{-1})$	10^{31}	10^{35}

$$b_1 = -\frac{3}{2} F_1^d A_{zz}$$

Very Unexpected Result

$$\int b_1(x)dx = 0$$

if the sea quark tensor polarization vanishes

$$\int_{0.0002}^{0.85} b_1(x)dx = 0.0105 \pm 0.0034 \pm 0.0035$$

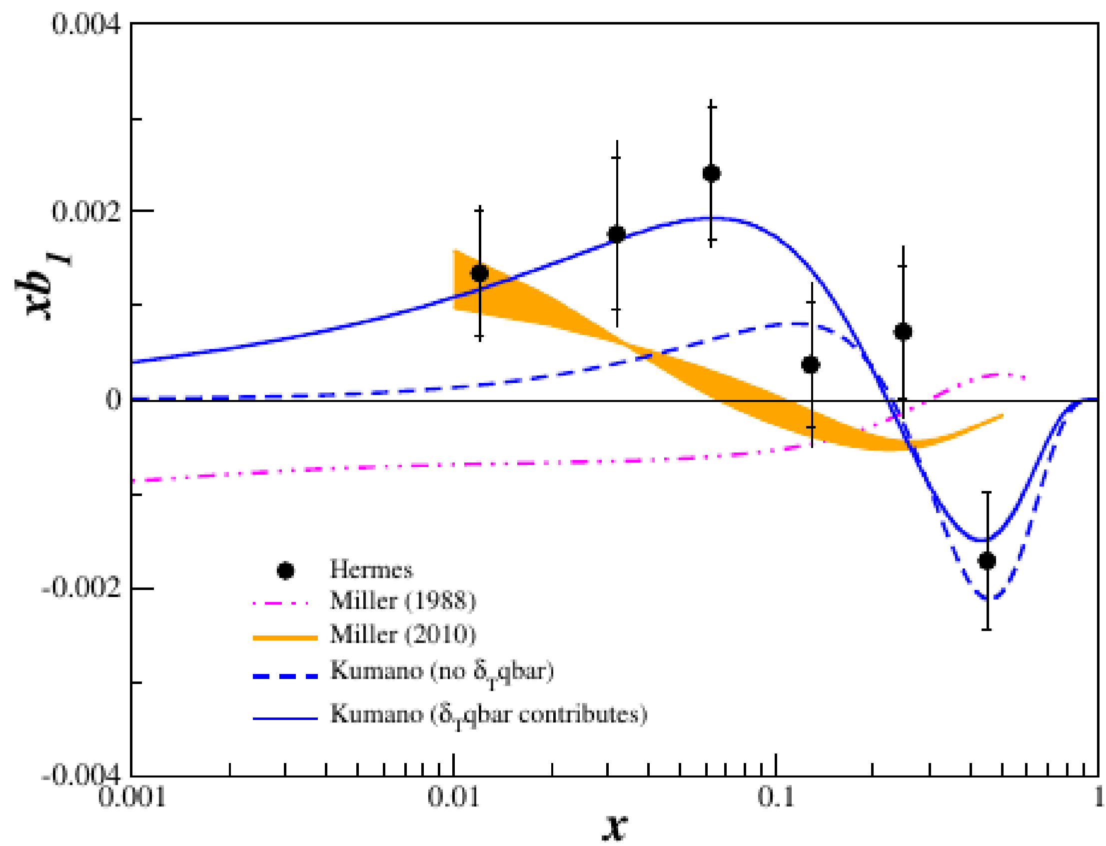

Efremov and Teryaev (1982, 1999)

Gluons (spin 1) contribute to both moments

Quarks satisfy the first moment, but

Gluons may have a non-zero first moment!

2nd moment more likely to be satisfied experimentally since the collective glue is suppessed compared to the sea

Study of b_1 allows to discriminate between deuteron components with different spins (quarks vs gluons)

no conventional nuclear mechanism can reproduce the Hermes data

Hidden Color

G. Miller **PRC89 (2014) 045203**

"Pionic and Hidden-Color, Six-Quark Contributions to the Deuteron **b1** Structure Function"

10% probability of tunneling transition

$$|6q\rangle = \sqrt{\frac{1}{9}}|NN\rangle + \sqrt{\frac{4}{45}}|\Delta\Delta\rangle + \sqrt{\frac{4}{5}}|CC\rangle$$

Nucleon-Nucleon — Delta-Delta — Hidden Color

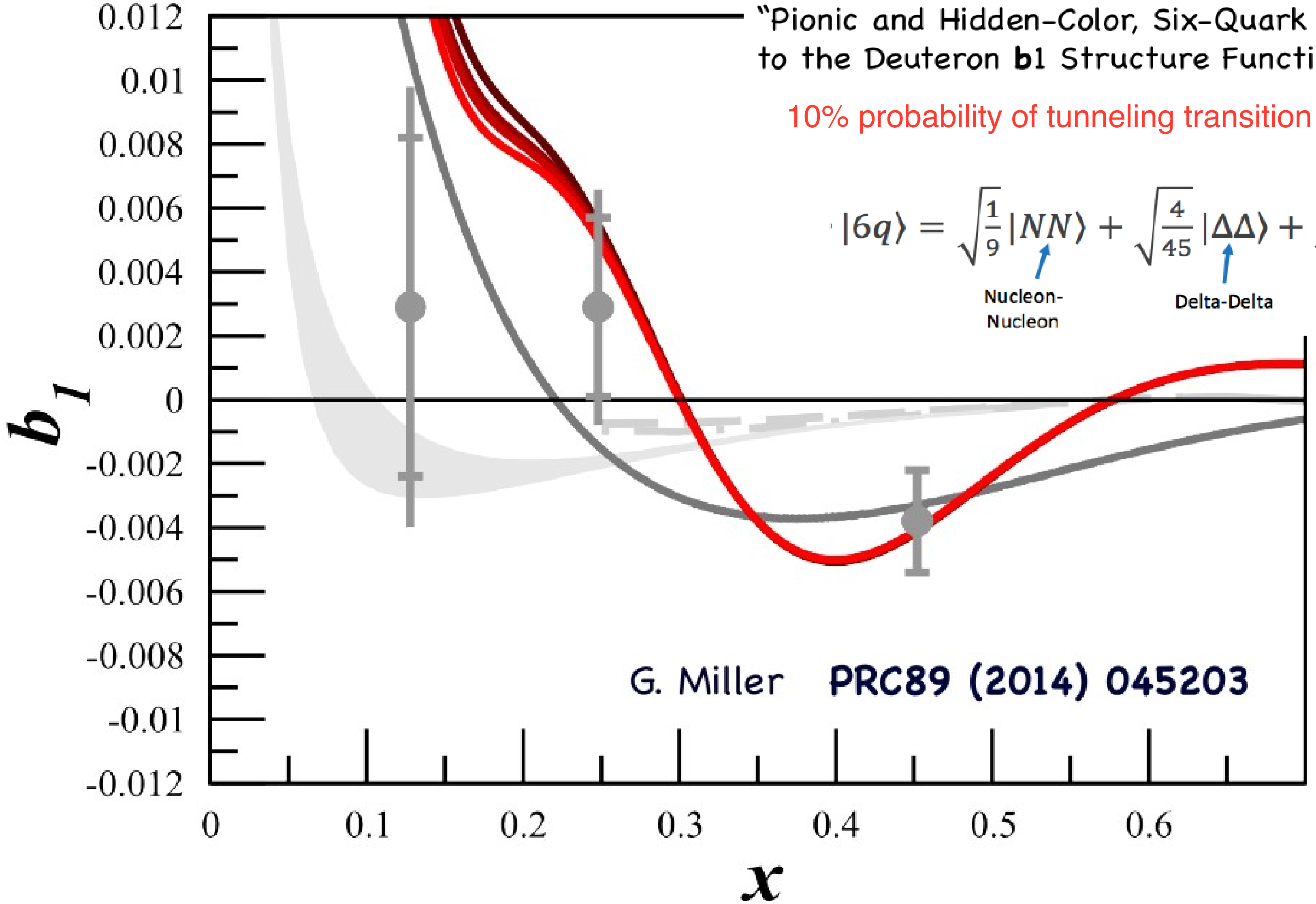

Hidden Color

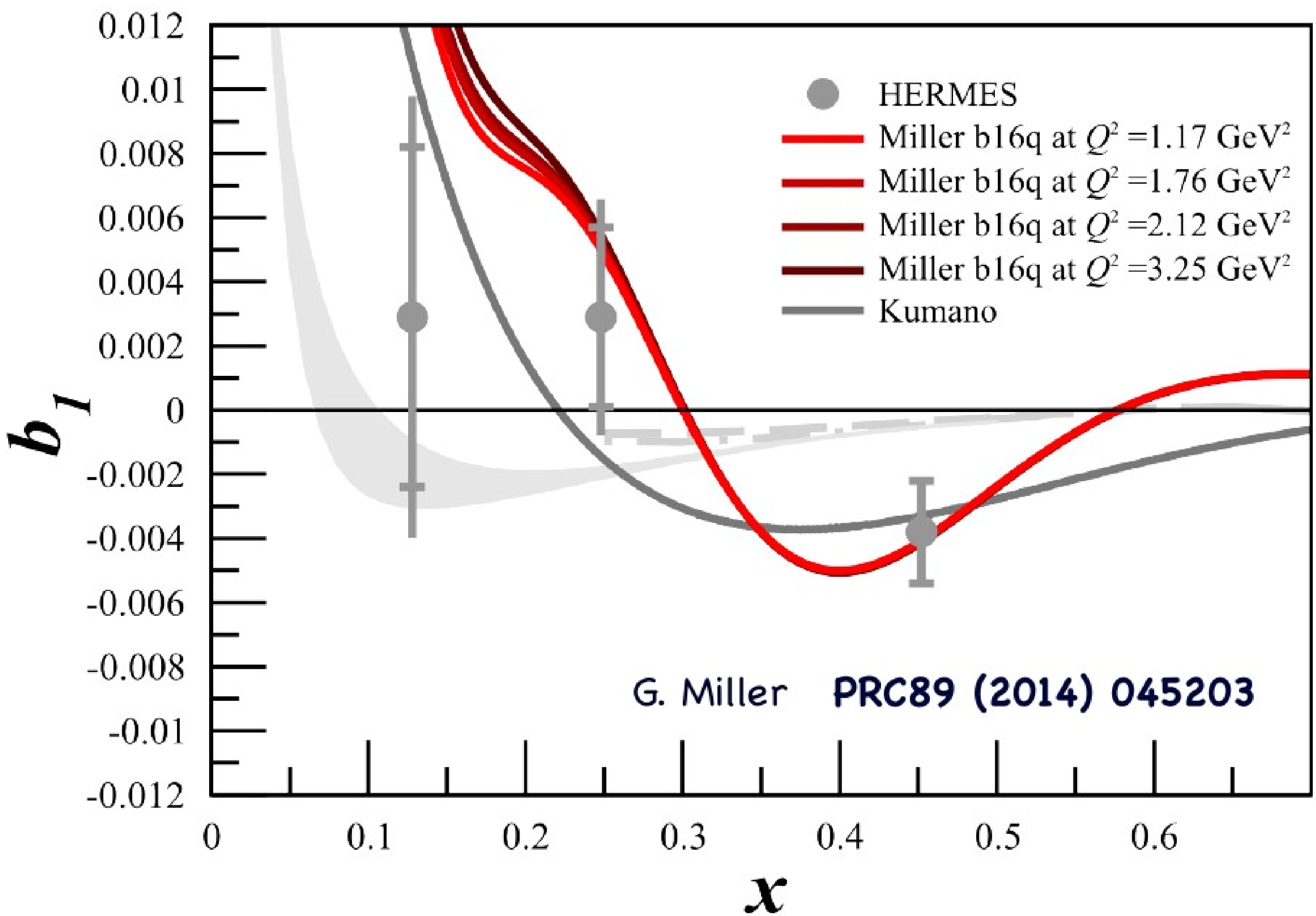

Hall C

Proposed at Jefferson Lab Hall C
PAC-40 conditionally approved with A- rating

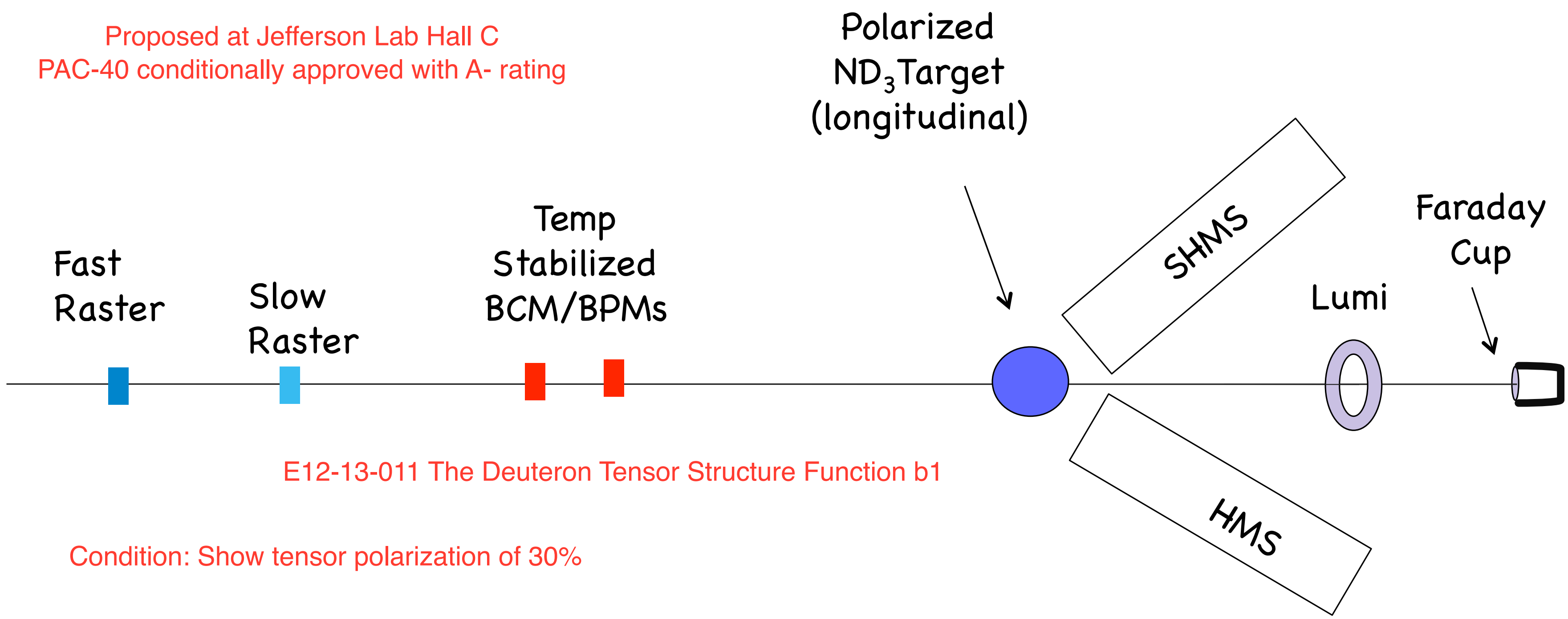

E12-13-011 The Deuteron Tensor Structure Function b1

Condition: Show tensor polarization of 30%

E12-15-005 Tensor Asymmetry Quasielastic Region
HIGS-P-12-16 Tensor Analyzing Power in Deuteron Photodisintegration

---

Unpolarized Beam : 115 nA

UVa/JLab Polarized Target

$\mathcal{L}=10^{35}$

Magnetic Field Held Along Beam Line at all times

Systematics

$\delta\xi$

Charge Determination
< 2×10^{-4}, mitigated by thermal isolation of BCMs and addition of 1 kW Faraday cup

Luminosity
< 1×10^{-4}, monitored by Hall C lumi

Target dilution and length   step like changes observable in polarimetry
< 1×10^{-4}

Beam Position Drift effect on Acceptance
< 1×10^{-4} (we can control the beam to 0.1 mm, raster over 2cm diameter)

Effect of using polarized beam
< 2.2×10^{-5}, using parity feedback

Impact on the observable

False asymmetry suppressed by degree of polarizaton

$$\delta A_{zz} = \pm \frac{2}{f P_{zz} \sqrt{N_{cycles}}} \delta\xi$$

Projected Results

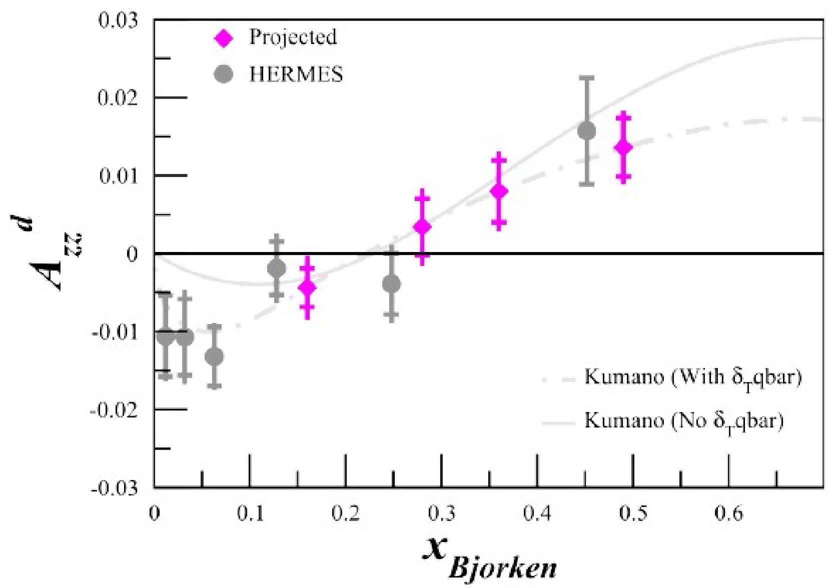

P_{zz}=20%

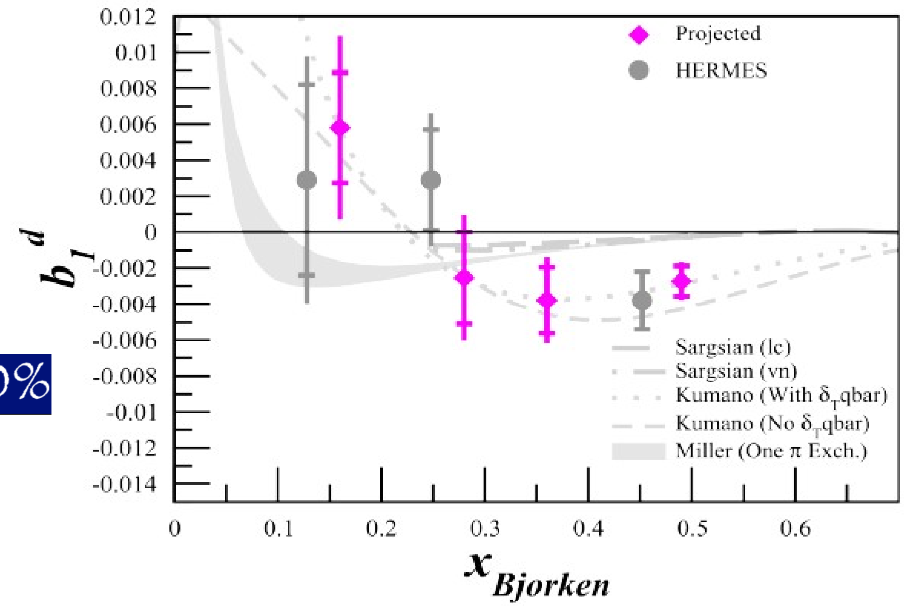

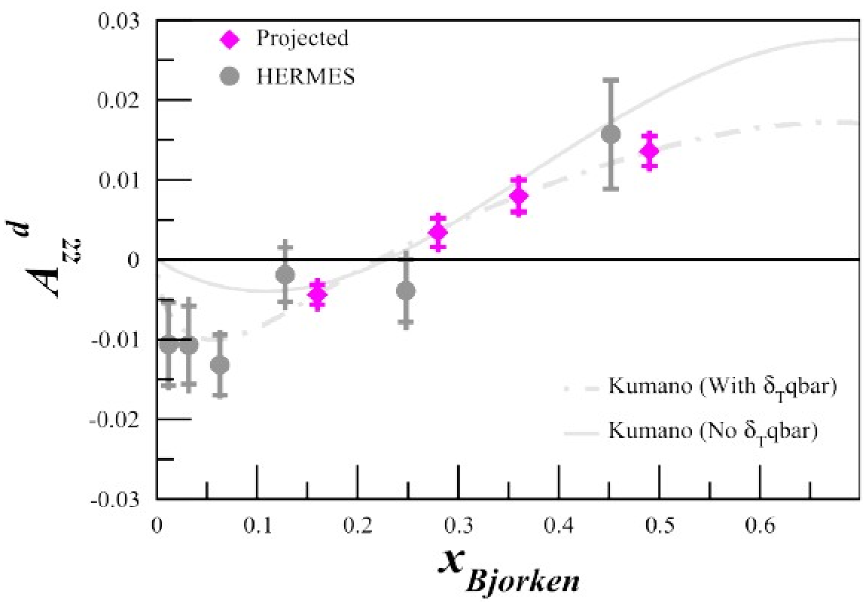

P_{zz}=40%

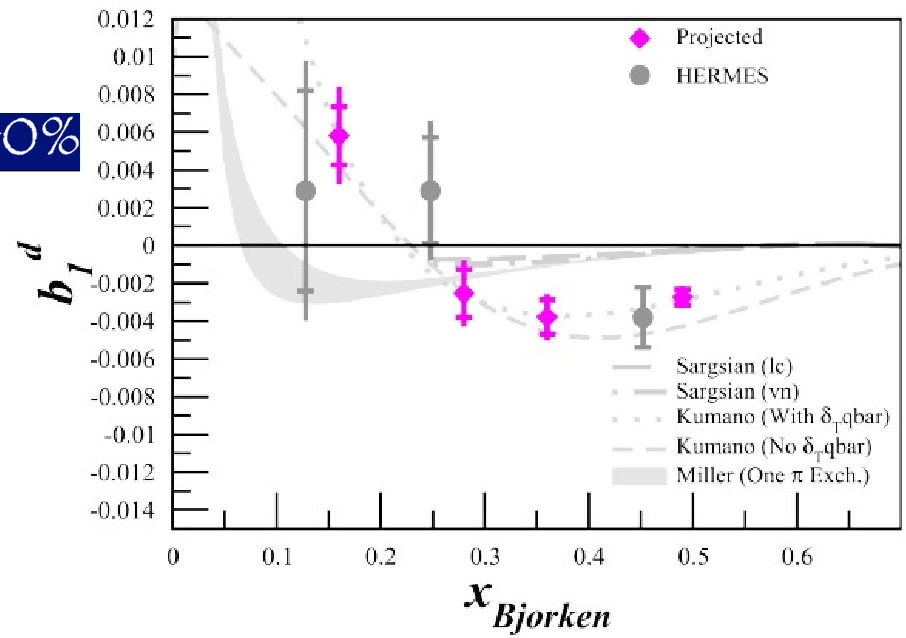

The DY Effort

- 2010 First Discussion with Kumano
  - Possibility of DY access PRD 59 (1999) 094026
    PRD 60 (1999) 054018
- Sparked Interest
  - S. Kumano, S. Phys.Rev. D82 (2010) 017501
  - S. Kmano 2014 J. Phys.: Conf. Ser. 543 012001
  - S. Kumano et al. Phys.Rev. D94 (2016) no.5, 054022
  - S. Kumano arXiv:1702.01477
  - S. Kumano arXiv:1902.04712

Drell-Yan Process

$$P + D \rightarrow \gamma^* \rightarrow \mu^- \mu^+ + X$$

$E_p = 120\ GeV$

$s = (p_1 + p_2)^2 = M_p^2 + M_d^2 + 2 M_d E_p$

$Q^2 = x_1 x_2 s$

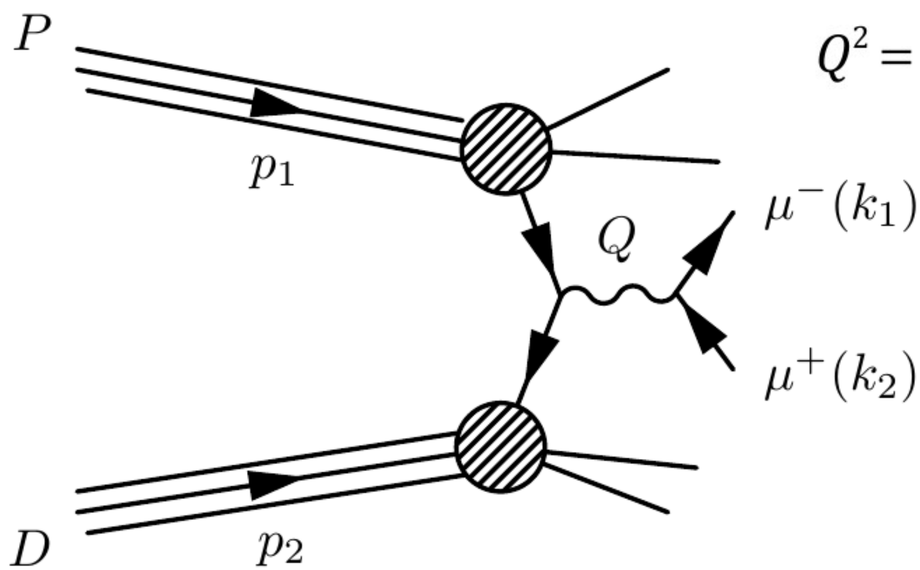

$$W_{\mu\nu} = \int \frac{d^4\xi}{(2\pi)^4} e^{iQ\xi} \left\langle P_1 S_1 P_2 S_2 \middle| J_\mu(0) J_\nu(\xi) \middle| P_1 S_1 P_2 S_2 \right\rangle$$

DY-Tensor Polarization

There are 108 structure functions for the hadron tensor of unpolarized proton-polarized deuteron Drell-Yan Process, and the spin asymmetry A_{UQ0} is measured with the tensor polarized deuteron.

$$A_{UQ_0} = \frac{1}{2\langle\sigma\rangle}[\sigma(\bullet,0) - \frac{\sigma(\bullet,+1)+\sigma(\bullet,-1)}{2}]$$

PRD 59 (1999) 094026
PRD 60 (1999) 054018

In Parton Model

$$A_{UQ_0} = \frac{\sum_i e_i^2(q_i(x_1)\delta_T\bar{q}_i(x_2)+\bar{q}_i(x_1)\delta_T q_i(x_2))}{2\sum_i e_i^2(q_i(x_1)\bar{q}_i(x_2)+\bar{q}_i(x_1)q_i(x_2))}$$

Update to Model

The spin asymmetry A_{UQ0} will indicate that existence of tensor –polarized distributions $\delta_T q$ and $\delta_T \bar{q}$, which are only available in D-wave deuteron. In experiment, the tensor –polarized distributions have been confirmed by Hermes measurements for b_1 of electron-deuteron DIS.

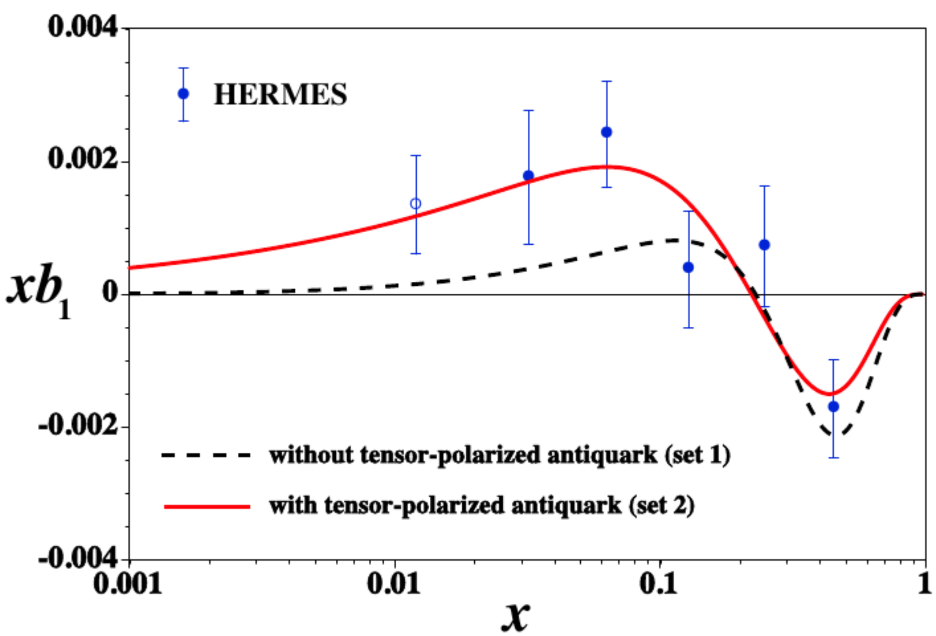

Set-1 results of xb_1 can not explain the Hermes data at small x (x<0.1).

Set-2 results can fit the data well enough.

It is better to consider the antiquark tensor-polarized distributions at Q^2=2.5 GeV^2.

Update to Model

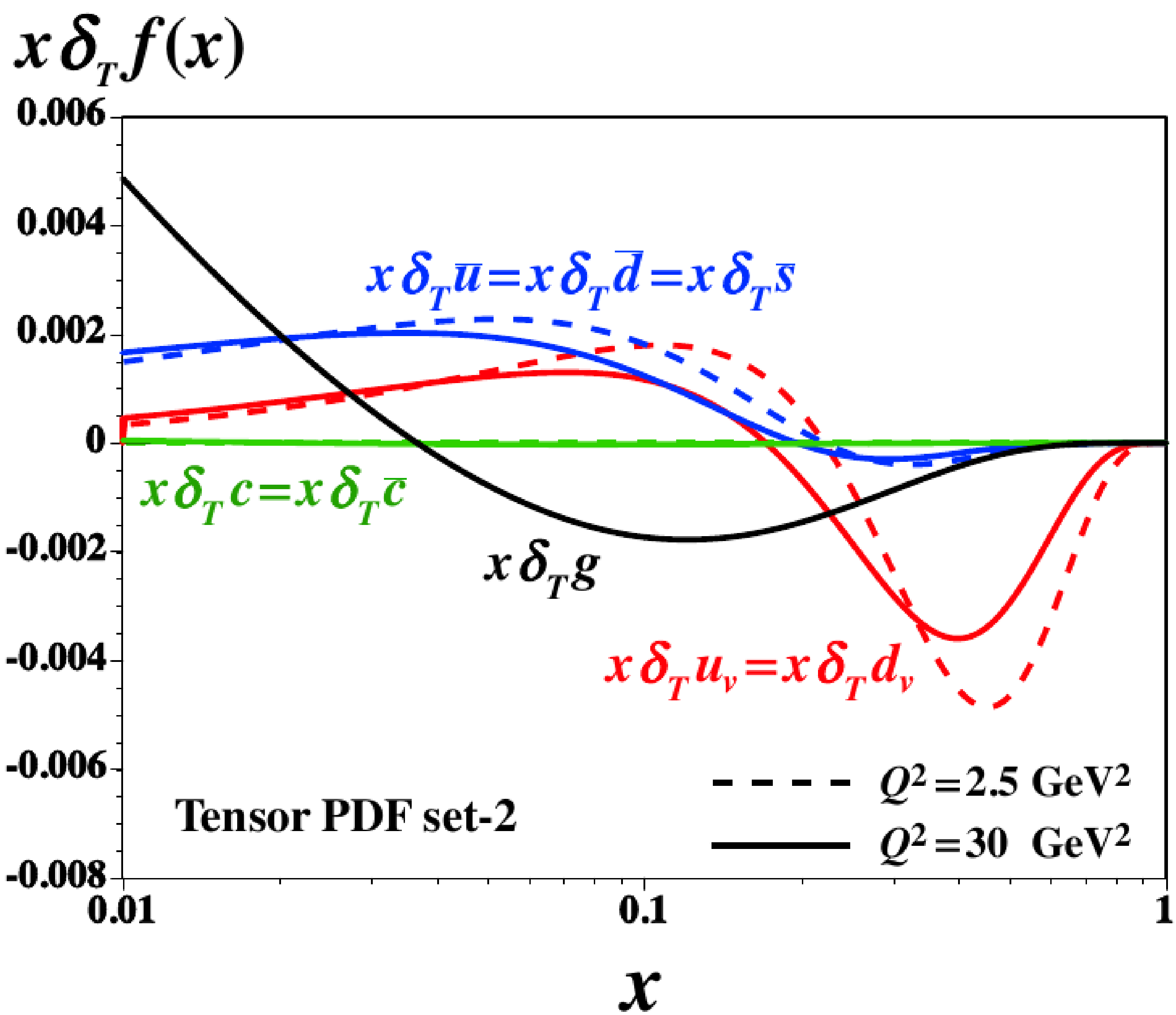

symmetry for antiquarks

$\delta_T\bar{u} = \delta_T\bar{d} = \delta_T\bar{s} \neq \delta_T\bar{c}$

The tensor-polarized PDFs are evolved to a FNAL

Notice significant tensor-polarized gluon distribution

DY is more sensitive to the Sea

Update to Model

set-2 (Includes Sea)

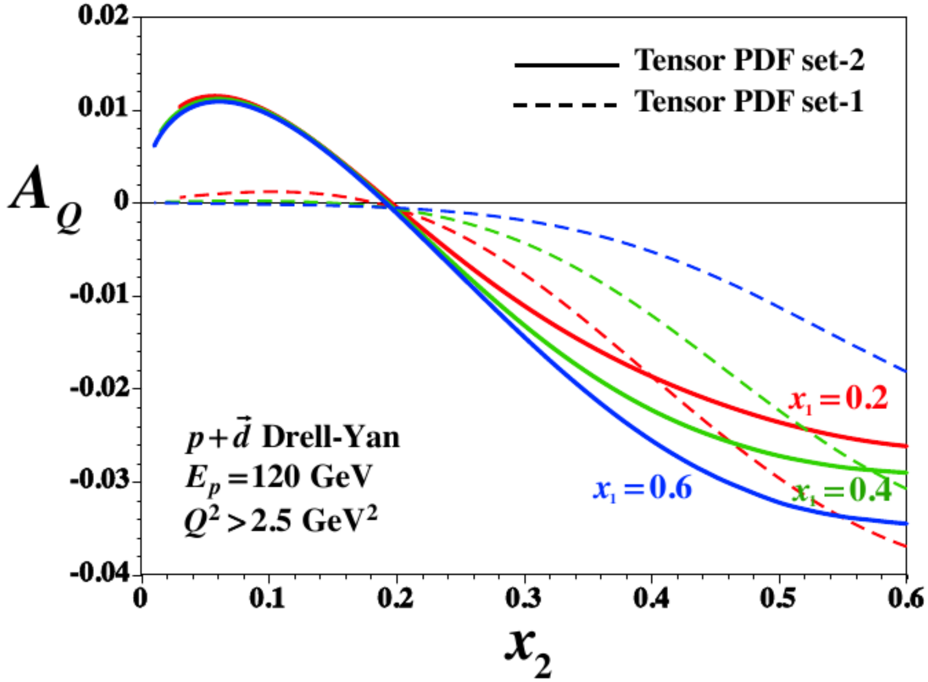

In the figure, tensor-polarized asymmetry A_Q is shown at typical values of x_1=0.2, 0.4 and 0.6.

$$A_Q(x_1, x_2) = 2A_{UQ_0}(x_1, x_2)$$

$$A_{UQ_0} = \frac{\sum_i e_i^2 (q_i(x_1)\delta_T \bar{q}_i(x_2) + \bar{q}_i(x_1)\delta_T q_i(x_2))}{2\sum_i e_i^2 (q_i(x_1)\bar{q}_i(x_2) + \bar{q}_i(x_1) q_i(x_2))}$$

The values of set-1 and set-2 are both a few percent.
The set-1 results are so different from those of set-2 at small region of x_2, and this is because that antiquark tensor-polarized distributions are more important when x_2 is small.
The set-2 results should be more reliable, since the tensor-polarized distributions can also explain the Hermes data well.

Tensor Polarization

Spin-1/2 system in B-field leads to 2 sublevels due to Zeeman interaction

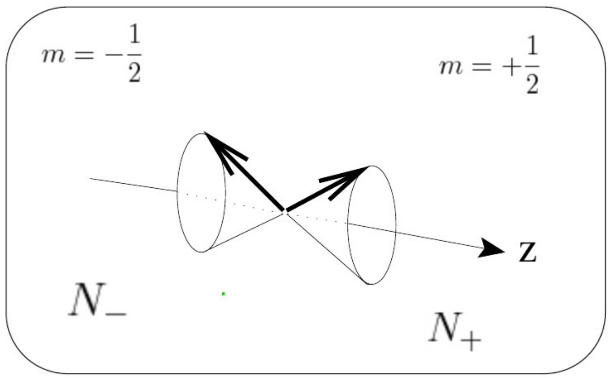

$$P_z = \frac{N_+ - N_-}{N_+ + N_-}$$

$-1 < P_z < +1$

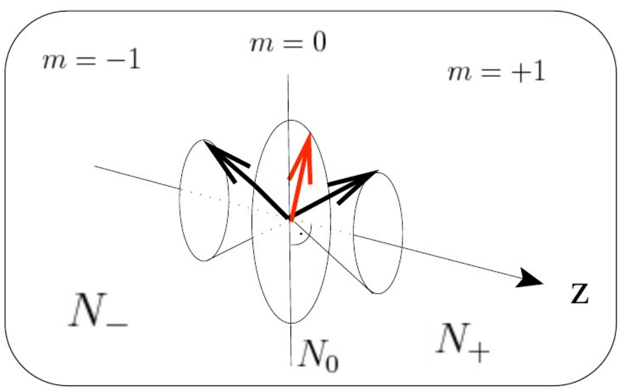

$$P_z = \frac{N_+ - N_-}{N_+ + N_-}$$

$$P_{zz} = \frac{(N_+ - N_0) - (N_0 - N_-)}{N_+ + N_0 + N_-} = \frac{(N_+ + N_-) - 2N_0}{N_+ + N_0 + N_-}$$

For Spin-1 Target

- Three magnetic sublevels
- Two transitions +1 → 0 and 0 → -1
- Deuteron electric dipole moment eQ
- Interaction with electric field gradient

Novel Targets for Novel Physics

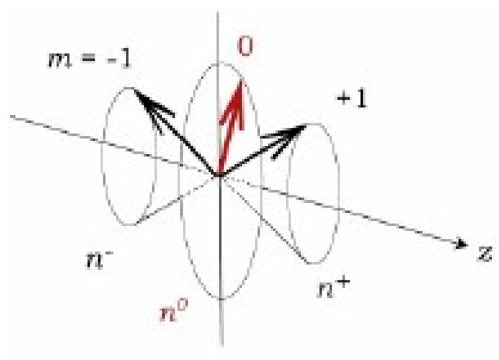

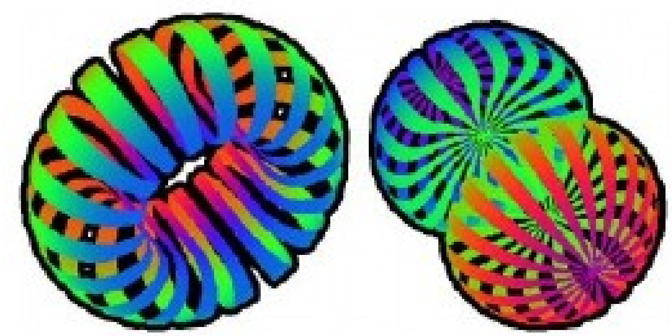

Densities of the deuteron in its two spin projections $I_z = 0$ and $I_z = 1$

$$P = \frac{n_+ - n_-}{n_+ + n_- + n_0} \quad (-1 < P_z < 1)$$

$$P_{zz} = \frac{n_+ - 2n_0 + n_-}{n_+ + n_- + n_0} \quad (-2 < P_{zz} < 1)$$

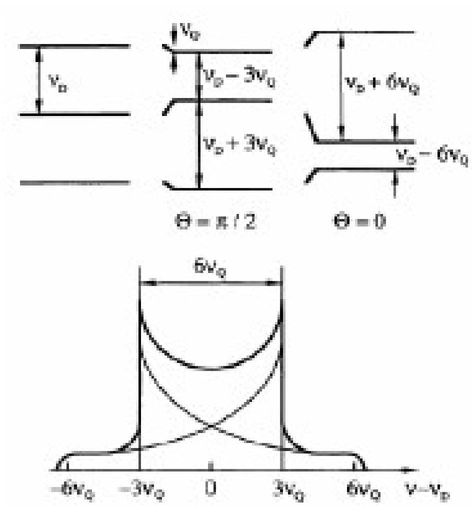

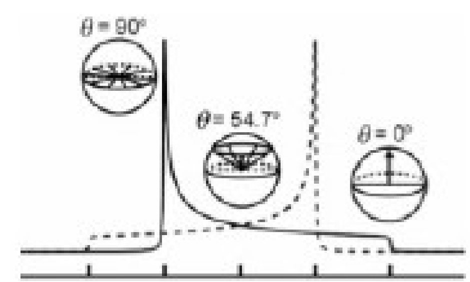

- Using Spin-1 (ND_3) Target
- Three Magnetic substates (+1,0,-1)
- Two Transitions ($+1 \rightarrow 0$) and ($0 \rightarrow -1$)
- Deuterons electric quadrupole moment eQ
- Interacts with electric field gradients within lattice

Options of Enhancement

- Increase the B-Field (Longitudinally Polarized)
- Decrease Temperature
- Manipulate using AFP

  Smooth modulation passage over the frequency domain in a time shorter than relaxation rates
- RF CW-NMR Manipulation

  Selective Semisaturation: SSS

  MAS + Slow Tilted MAS

Natural Equilibrium Polarization

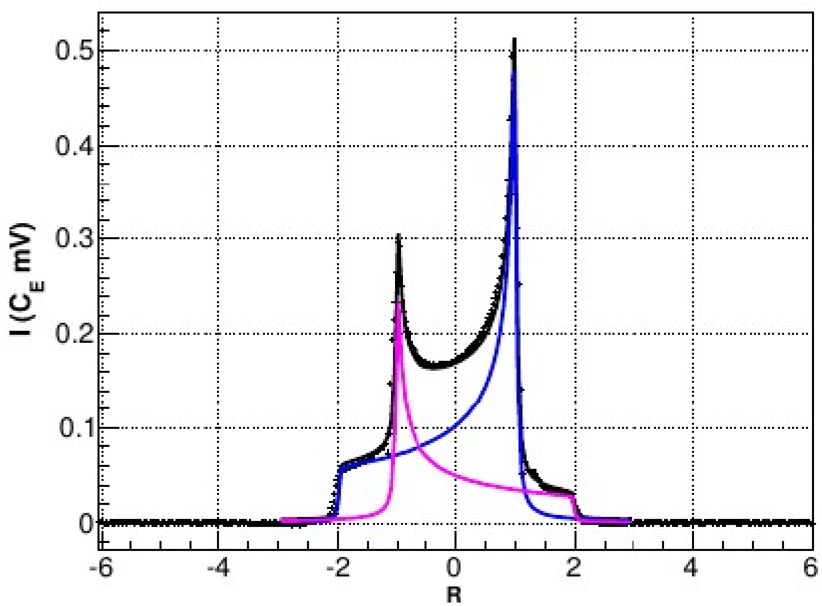

$R = \frac{\omega - \omega_d}{3\omega_q}$

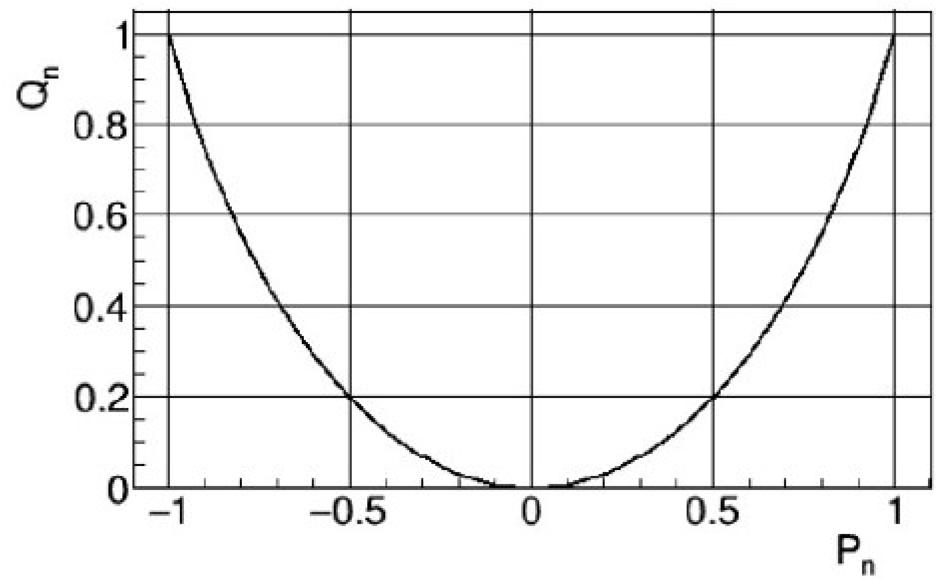

$$P_n = \frac{2\hbar}{g^2\mu_N^2\pi N}\int_{-\infty}^{\infty}\frac{3\omega_Q\omega_D}{3R\omega_Q+\omega_D}\chi''(R)dR$$
$$= \frac{1}{C_E}\int_{-\infty}^{\infty} I_+(R)+I_-(R)dR,$$

$$Q_n = (I_+ - I_-)/C_E$$

$$Q_n = 2 - \sqrt{4-3P_n^2}$$

- Under Boltzmann equilibrium the relationship between vector and tensor polarization always exists
- Under this same condition the Height of each peak maintains a relationship to each other that contains all polarization information
- The ratio of the peak intensities can be used to calculate relative population in each magnetic sub-level

Natural Equilibrium Polarization

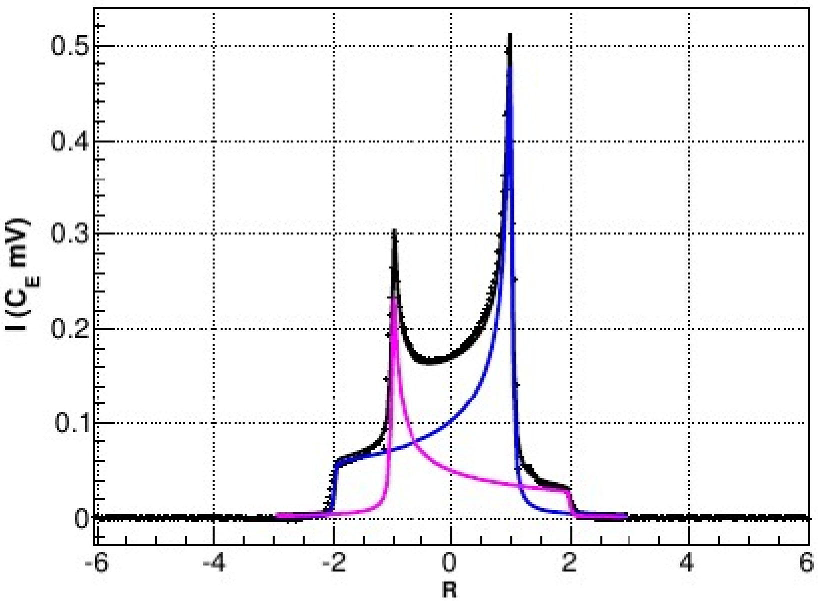

$R = \frac{\omega - \omega_d}{3\omega_q}$

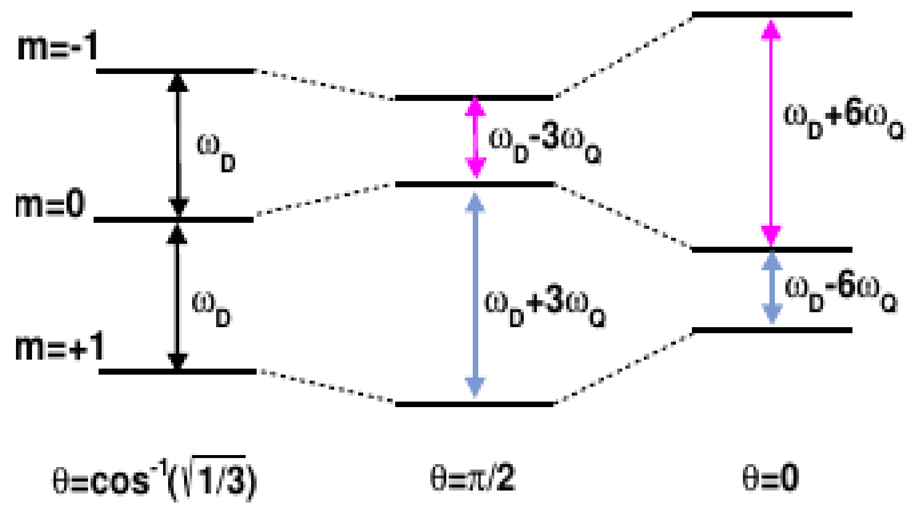

$$P_n = \frac{2\hbar}{g^2\mu_N^2\pi N}\int_{-\infty}^{\infty}\frac{3\omega_Q\omega_D}{3R\omega_Q+\omega_D}\chi''(R)dR$$
$$= \frac{1}{C_E}\int_{-\infty}^{\infty} I_+(R)+I_-(R)dR,$$

$$Q_n = (I_+ - I_-)/C_E$$
$$= (a_+ - a_0) - (a_0 - a_-)$$

$$Q_n = 2 - \sqrt{4 - 3P_n^2}$$

- Under Boltzmann equilibrium the relationship between vector and tensor polarization always exists
- Under this same condition the Height of each peak maintains a relationship to each other that contains all polarization information
- The ratio of the peak intensities can be used to calculate relative population in each magnetic sub-level

Selective Semi-saturation

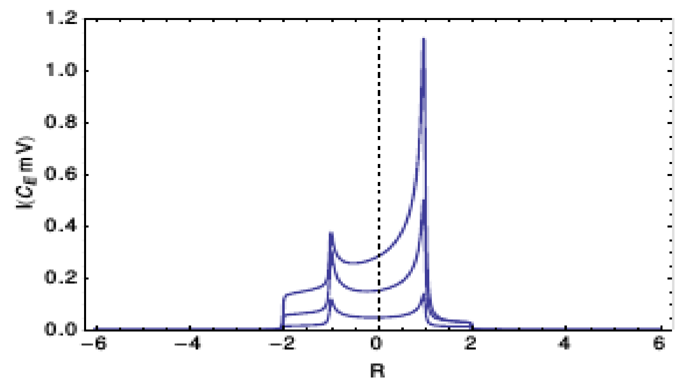

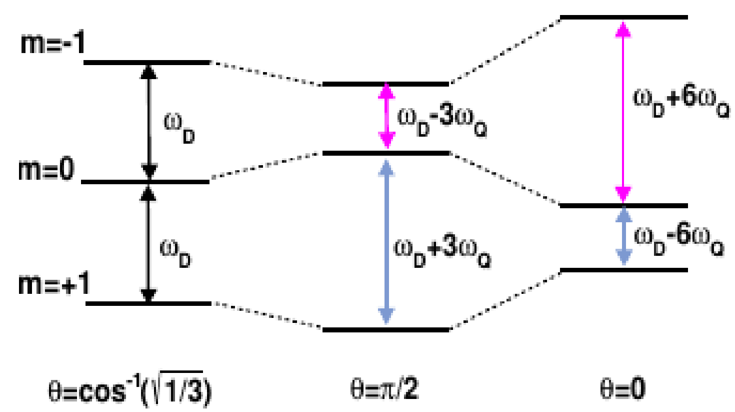

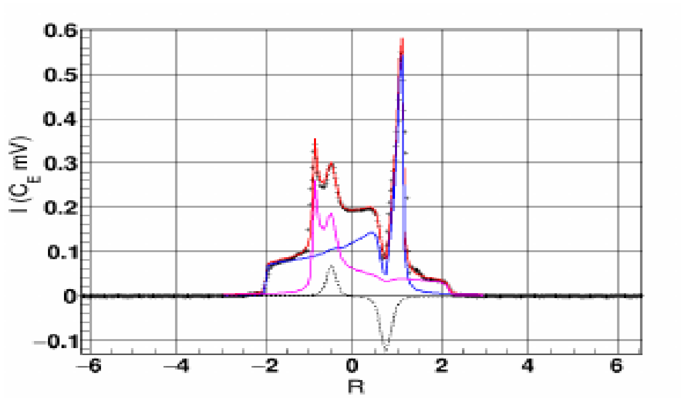

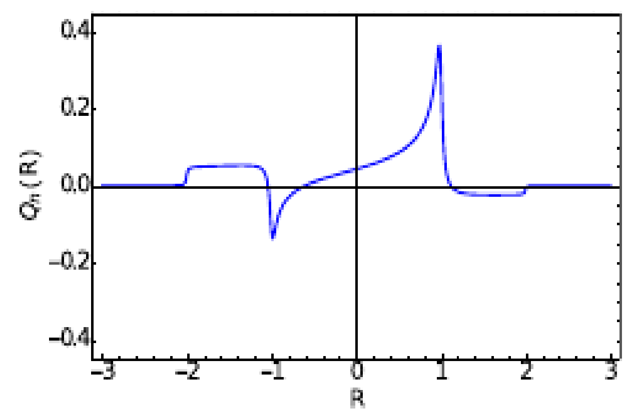

- Selective RF manipulation of the CW-NMR line
- Enhanced by mitigating the amplitudes below zero
- Can be implemented in parallel to DNP

Novel Targets for Novel Physics

RF Manipulation

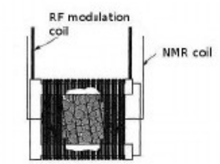

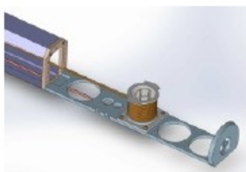

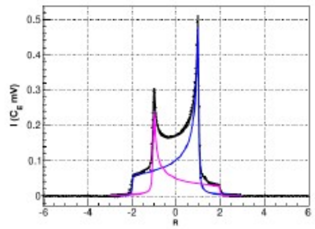

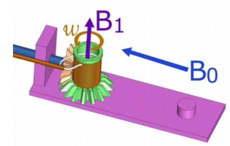

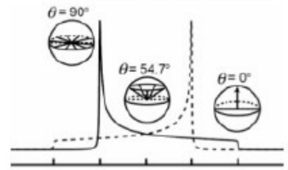

- RF irradiation at the Larmor frequency induces transitions between m=0 and other energy levels
- RF induced transitions at a single θ has a resulting effect on two positions in the line R and $-R$ through conservation of energy
- This can be implemented to shrink one transition lines area and enhancing the other resulting in tensor polarization manipulation

- Study Optimization Analytically
- Develop Simulated Lineshape under RF
  - Empirical info from RF-power profile and Spectral diffusion
  - Rate Eq for overlap ratio
  - Generate theoretical lineshape manipulated by RF
- Develop fitting procedure for measurement
  - Unique constraints for overlapping regions are provided by MC
  - Fit semi-saturated (optimized d-Ammonia)
  - Test measurements with specialized NMR and scattering experiments
- Further Optimized Enhancement
  - Slow Perpendicular Rotation with semi-saturating RF
  - Heavily Reliant on MC for measurements
  - Tested with d-but. but not yet for ammonia

Novel Tensor Enhanced Target

Tensor Enhancement Mechanism for single position

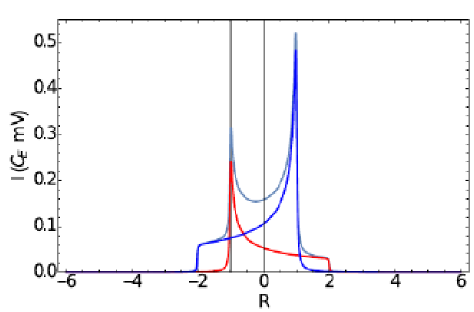

Selective Semi-saturation : Use power appropriate for position optimizing tensor polarization for all R

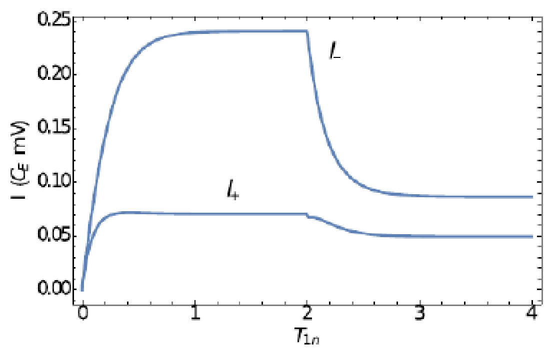

For peak Semi-saturation significant enhancement occurs by reduction of negative tensor polarization at R as well as adding to positive tensor polarization at $-R$

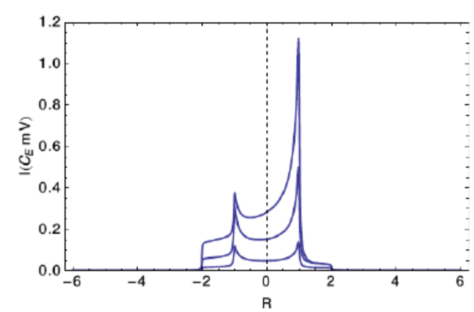

Simulated Examples of regular lineshape (13,42,78%)

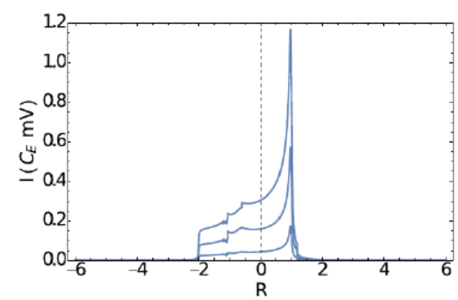

Examples Optimized Tensor Polarization Examples (1.3→5.4,13.6→23.8,52→58%)

Selective Semi-saturation
(or just hole burning)

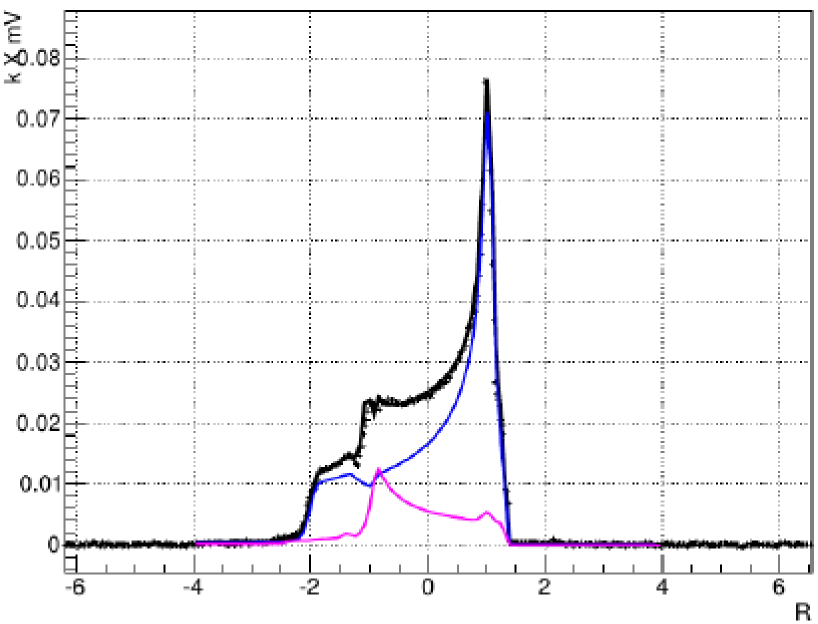

MC overlap with d-but. NMR experimental points (Pn=51→45,Qn:20→31%)

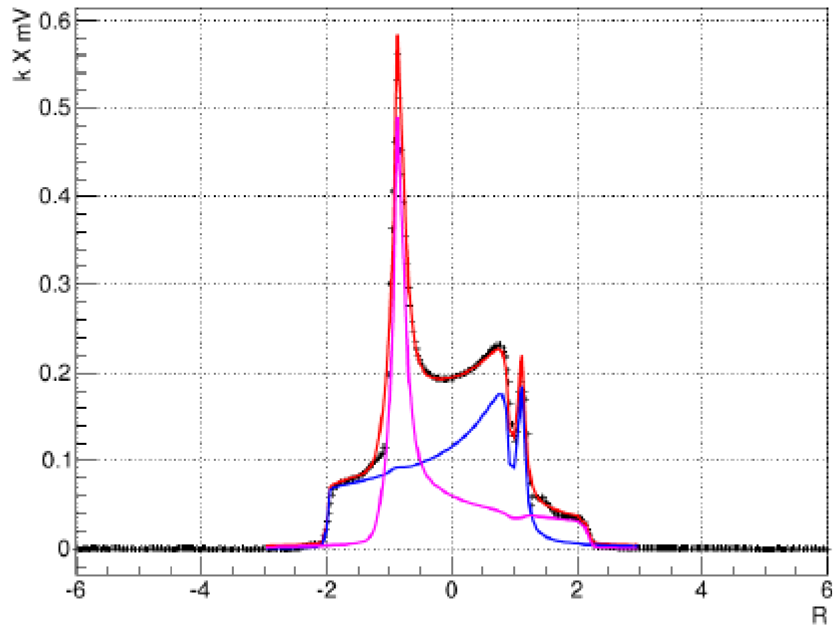

MC with fit and d-but. NMR experimental points (Pn=48→46,Qn:18→6%)

$$R = \frac{\omega - \omega_d}{3\omega_q}$$

DK Eur.Phys.J. A53 (2017) no.7, 155 arXiv:1707.07065

What Things Look Like

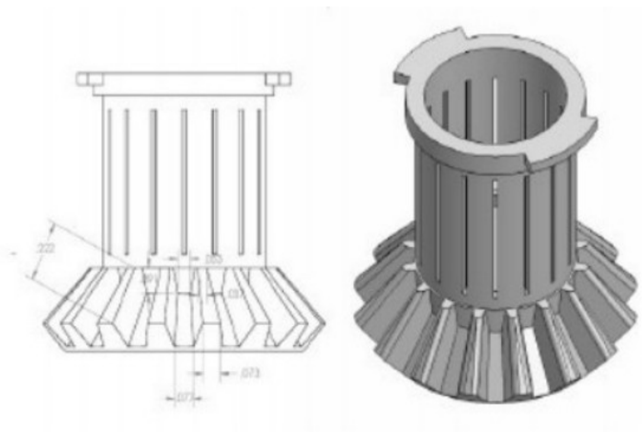

- Kel-F $(C_2ClF_3)_n$ cup and driving gear
- Motor outside cryostat
- NMR coil around cup
- Already used with several designs at UVA
- 1 Hz achieved with no problem
- Fixed beam spot

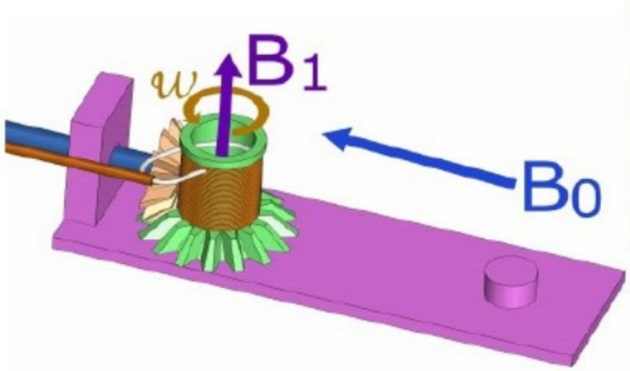

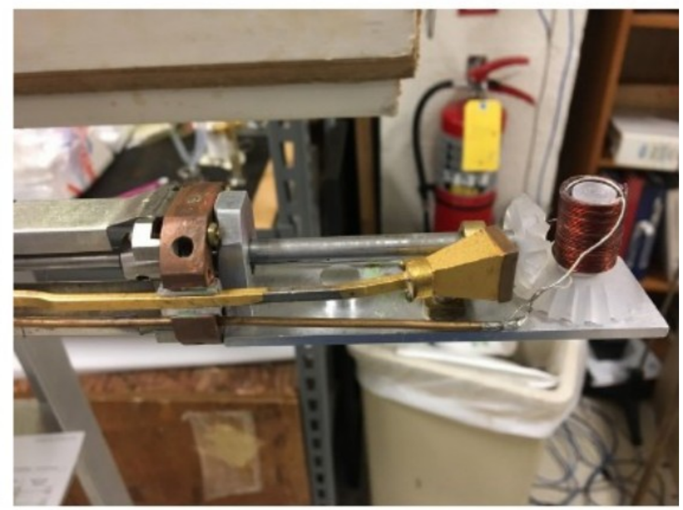

Rotating Target Concept

For dipolar couplings, the principal axis corresponds to the internuclear vector between the coupled spins

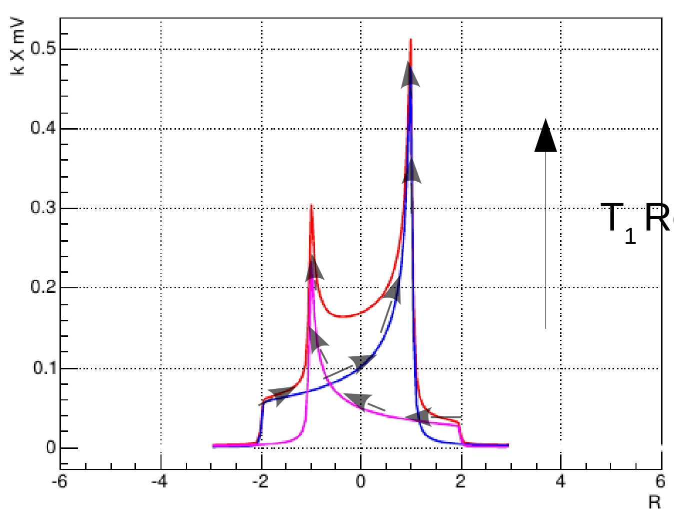

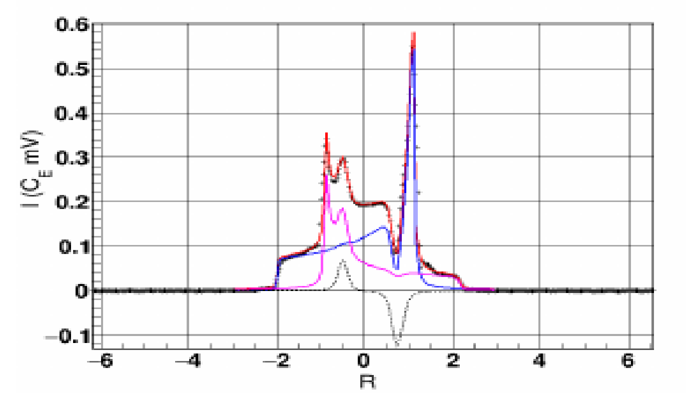

Rotational rate sill faster than T$_2$ Relaxation

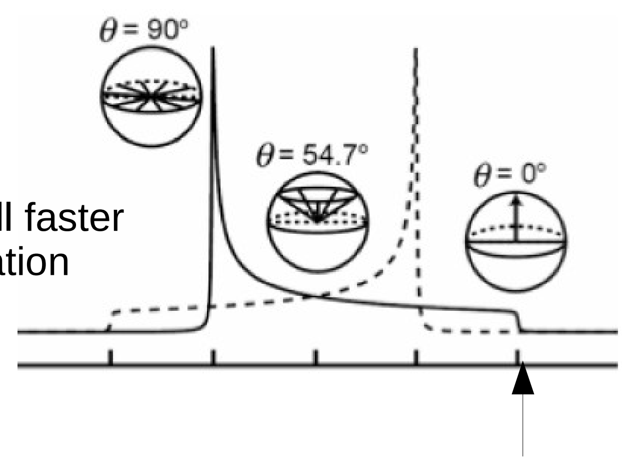

SSS with slow rotation

- Selective saturation/pumping while rotating
- Saturated domain moves with rotation
- Can enhance Q or go -Q

$$Q_n = (I_+ - I_-)/C_E$$
$$= (a_+ - a_0) - (a_0 - a_-)$$

MAS-PT

- Nuclear dipole-dipole interaction between magnetic moment average to zero at MA
- MA angle is a root of the second-order Legendre Polynomial P2 mitigating these local spin-spin interactions
- Tilted Slow MAS

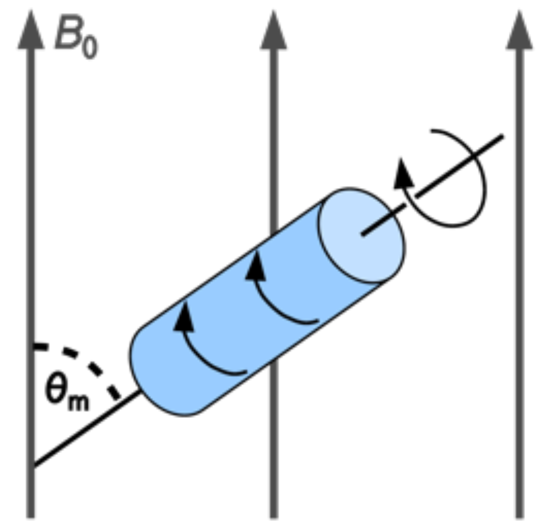

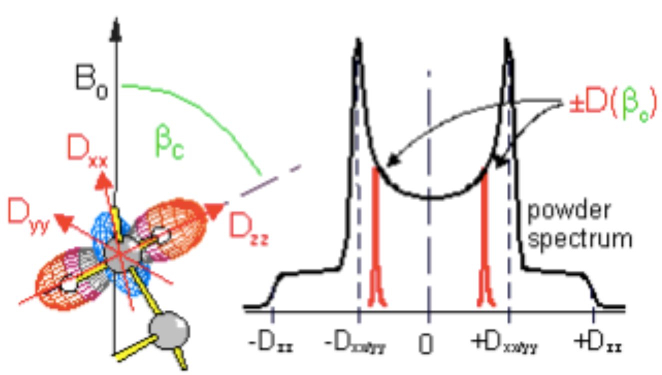

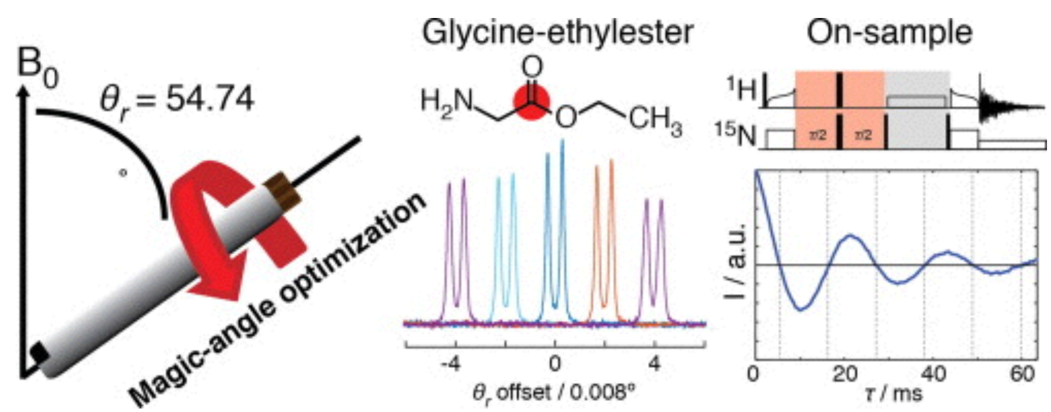

RF-Manipulated Signals

Fast target helicity flips through Adiabatic Fast Passage (AFP)

AFP at UVA

performed AFP on different materials (5T, 1K)

15NH3, D-butanol, butanol+tempo

preliminary results on flip efficiency

Table 1
Results from AFP experiments with various nuclei in differ[ent]
target materials

Nuclei	Substance dopant	e^- conc. (spins/g)	δP^{max}
^{1}H	1-butanol EHBA-Cr(V)	2.0×10^{19}	−0.76
^{7}Li ^{1}H	^{7}LiH (irradiated)	low	−0.90 −0.90
^{19}F ^{1}H	8-fluoro-1-pentanol TEMPO	1×10^{20}	−0.37 −0.40
^{2}H	1-butanol-d_{10} EHBA-Cr(V)-d_{22}	2.36×10^{19} 6.35×10^{19}	−0.92 −0.90

NIM 356 (1995) 108

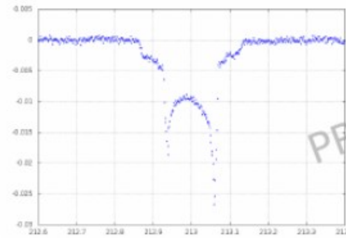

before

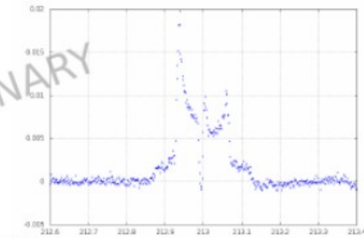

after

flip efficiency >0.8

15NH3

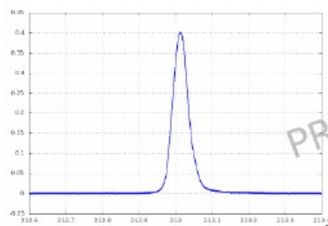

before

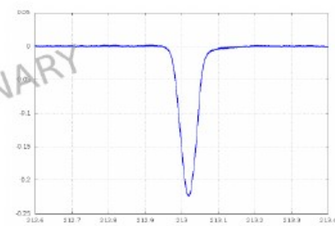

after

flip efficiency 0.55

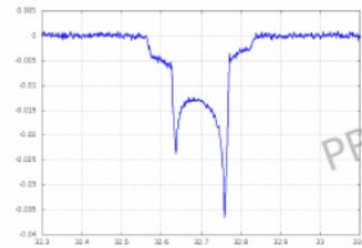

before

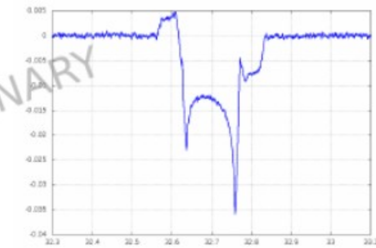

after

PRELIMINARY

AFP produces rotation of the macroscopic magnetization vector by sweeping through resonance in a short time compared to the relaxation time

- Set record for Tensor Polarization for Deuteron (d-b only) Q>31% @1K 5T
- Set record for AFP flip with Proton e>50% @ 1K 5T

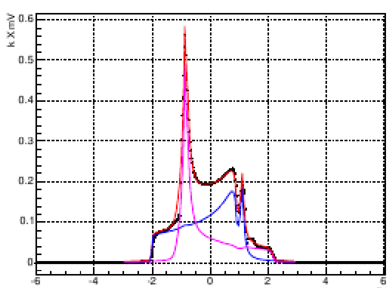

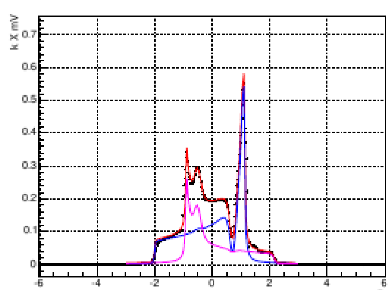

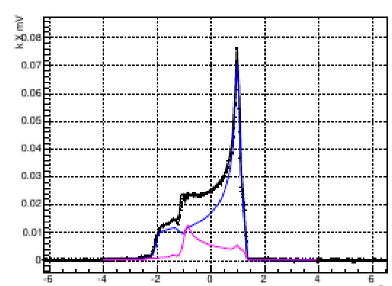

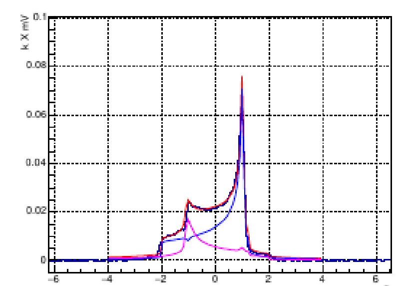

Achieved So Far

- Before recent research (1984): ~20%
- Recent studies SSS: (2014-2015): ~30%
- AFP with SSS (2016): ~34%
- Rotation with SSS: ~39%

DK **Eur. Phys. J. A (2017) 53: 155**
DK PoS, PSTP2015:014 (2016)
DK J.Phys.Conf.Ser., **543**(1):012015 (2014)
DK Int.J.Mod.Phys.Conf.Ser., **40**(1):1660105 (2016)

A Possible Fermilab Setup

Split Pair

Must be Longitudinal

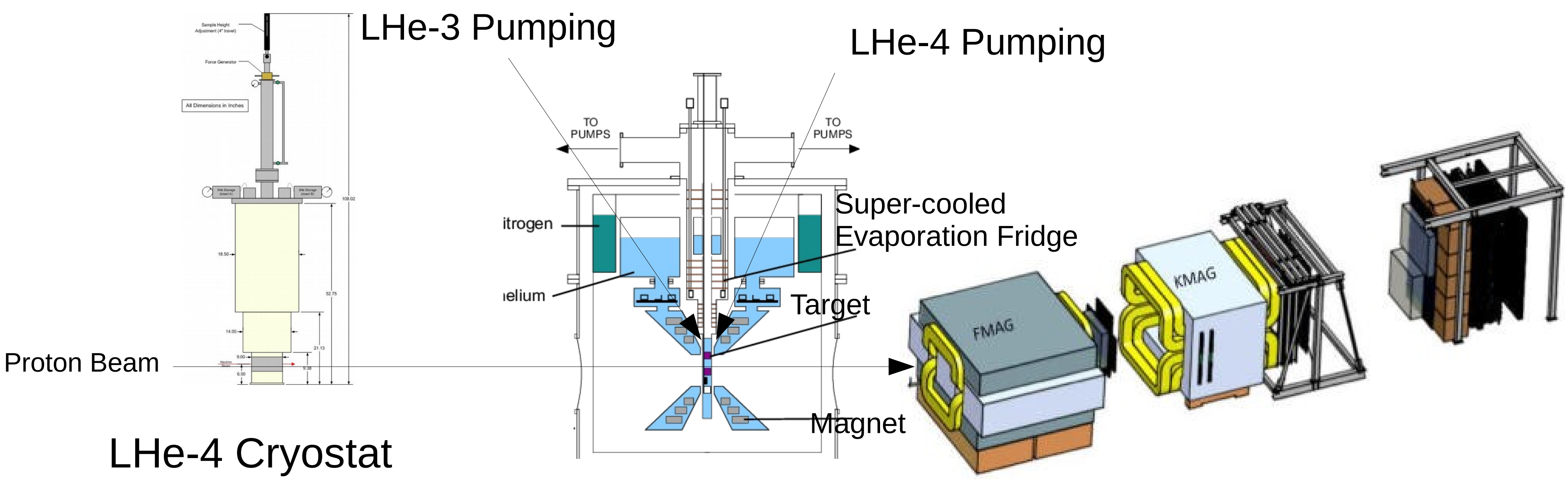

LHe-4 Cryostat

- No Field
- 4 K reservoir
- Hold ND3 with no Polarization

Supercooled He-4 System

- High Cooling Power
- Low Temp 0.4 K
- High ND3 Tensor Polarization ~70%

What to Add

- New Magnet
- New Fridge
- He-3 System
- Additional Pumps

A Possible Fermilab Setup

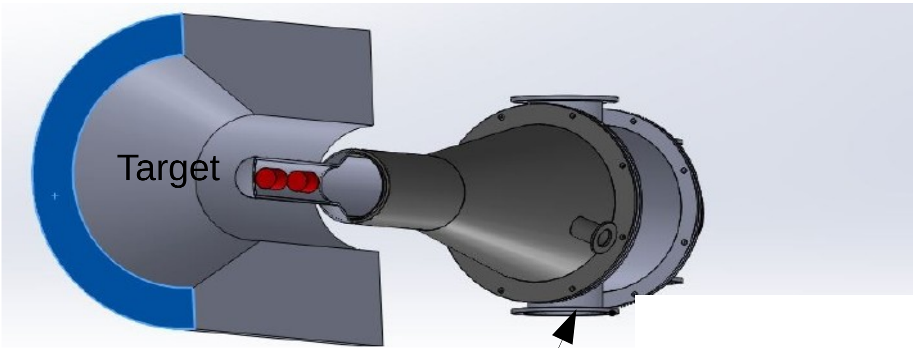

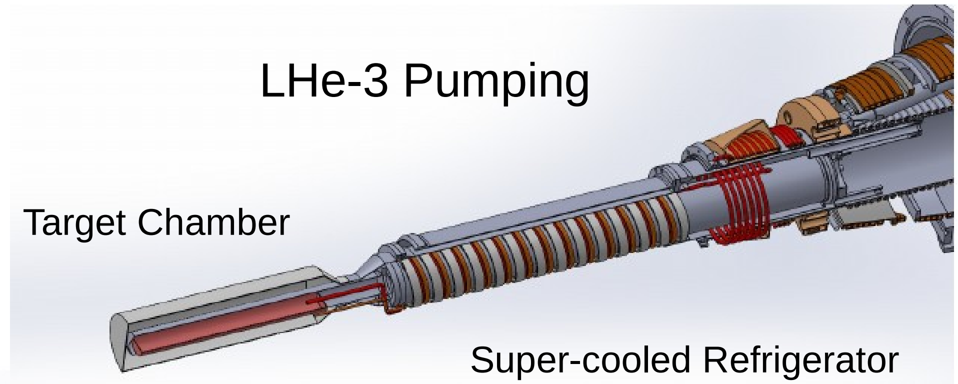

LHe-4 Pumping

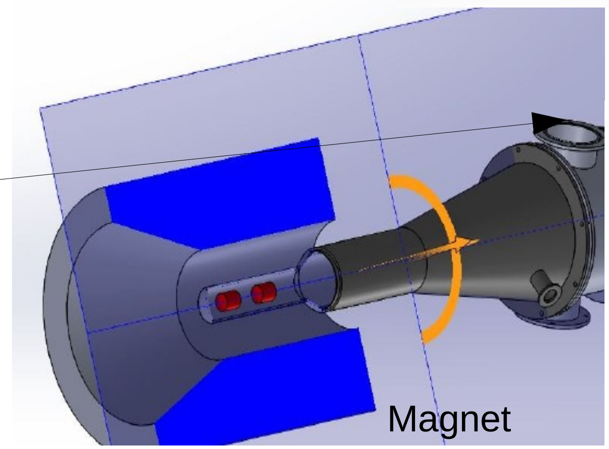

$$P \propto \exp\left(-\frac{L}{RT}\right)$$

Latent heat ^{4}He ~90 J/mol
Latent heat ^{3}He ~40 J/mol

Cooling power: exponentially small at low temperature
Pumping on ^{4}He T~1 K (normally down to 1.8 K)
Pumping on ^{3}He T~0.26 K (down to 0.3 K)

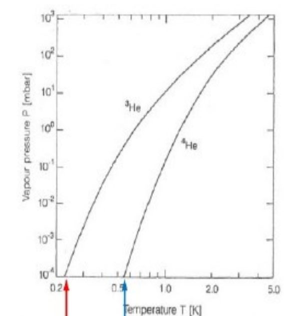

Fig.2.7. Vapour pressures of liquid ^{3}He and liquid ^{4}He

^{3}He-^{4}He dilution refrigeration: use the difference of the specific heats of the two phases (the enthalpy of mixing):

$$\Delta H \propto \int \Delta C dT \Rightarrow \dot{Q} \propto x\Delta H \propto T^2$$

Dilution refrigerator cooling power:~T^2

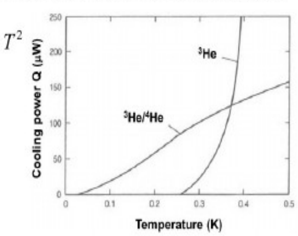

Super-cooled He-4 System

- High Cooling Power
- Low Temp 0.4 K
- High ND3 Tensor Polarization ~70%

High Cooling Power High Intensity Beams

Shifting Gears

Another Look at OAM

Ji

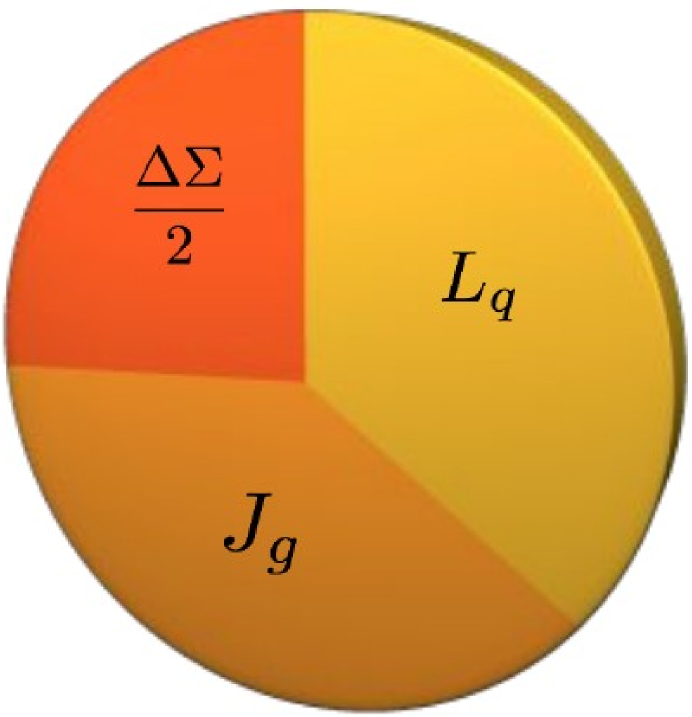

$$\frac{1}{2} = \frac{\Delta\Sigma}{2} + L_q + J_g$$

Jaffe Manohar

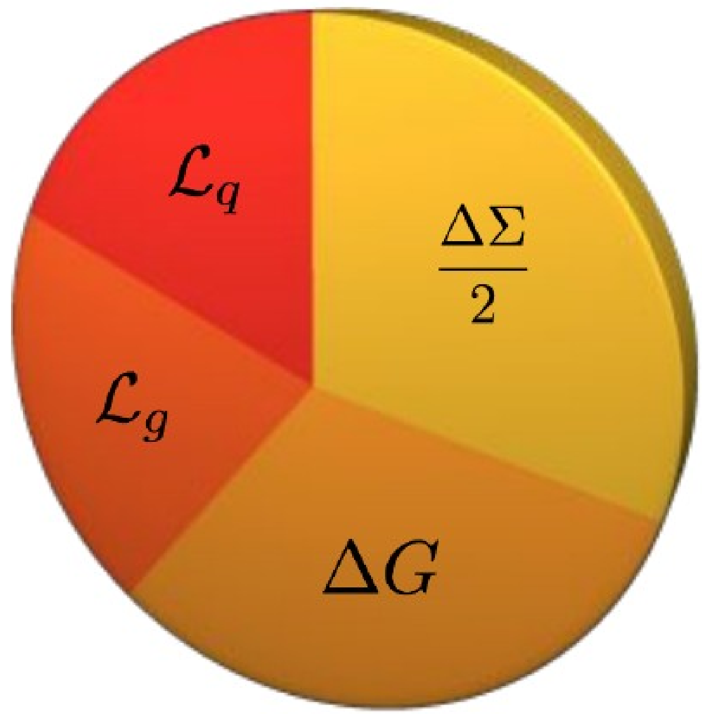

$$\frac{1}{2} = \frac{\Delta\Sigma}{2} + \mathcal{L}_q + \Delta G + \mathcal{L}_g$$

Another Look at OAM

Ji

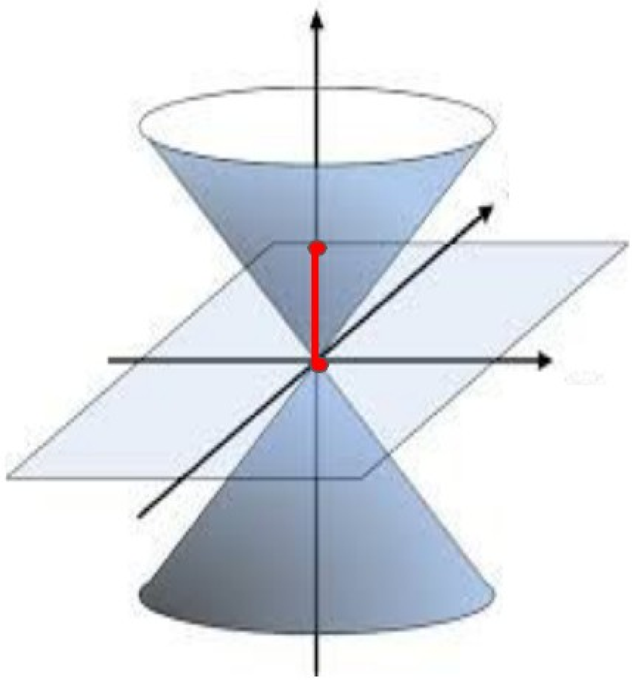

$$L_q = \int d^3r \langle P', \Lambda' | \overline{\psi} \gamma^+ \left(\vec{r} \times i\vec{D} \right) \psi | P, \Lambda \rangle$$

Jaffe Manohar

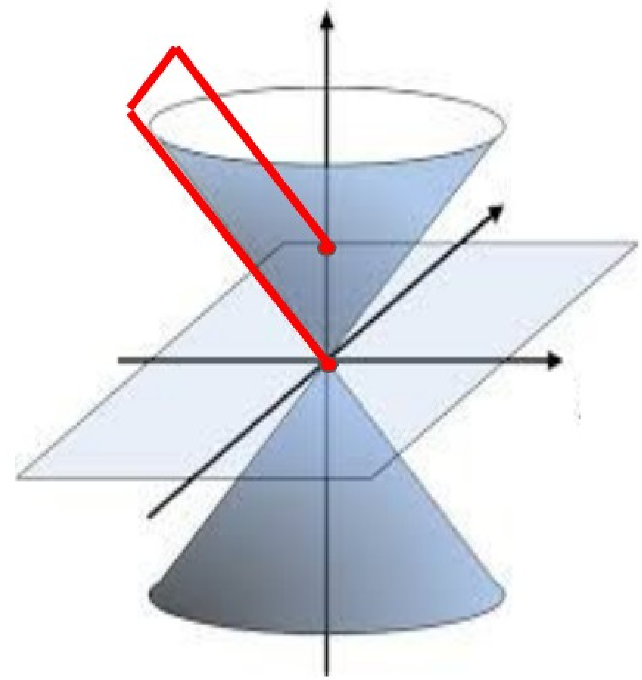

$$\mathcal{L}_q = \int d^3r \langle P', \Lambda' | \overline{\psi} \gamma^+ \left(\vec{r} \times i\vec{\partial} \right) \psi | P, \Lambda \rangle$$

Another Look at OAM

How do we describe the orbital angular momentum of the partons?

$$\vec{L} = \vec{r} \times \vec{p}$$

Classically

$$L_z^q = -\left(k_T \times b_T\right)_z^q$$

Partonic

b_T Relative average transverse position from the center of momentum of the system

k_T Relative average transverse momentum

$$l_z^q = \int dx d^2k_T d^2b_T \left(b_T \times k_T\right)_z^q \rho^{[\gamma^+]}(b_T, k_T, x)$$

$$l_z^q = -\int dx d^2k_T \frac{k_T^2}{M^2} F_{1,4}^q$$

Hierarchy of Hadron SF

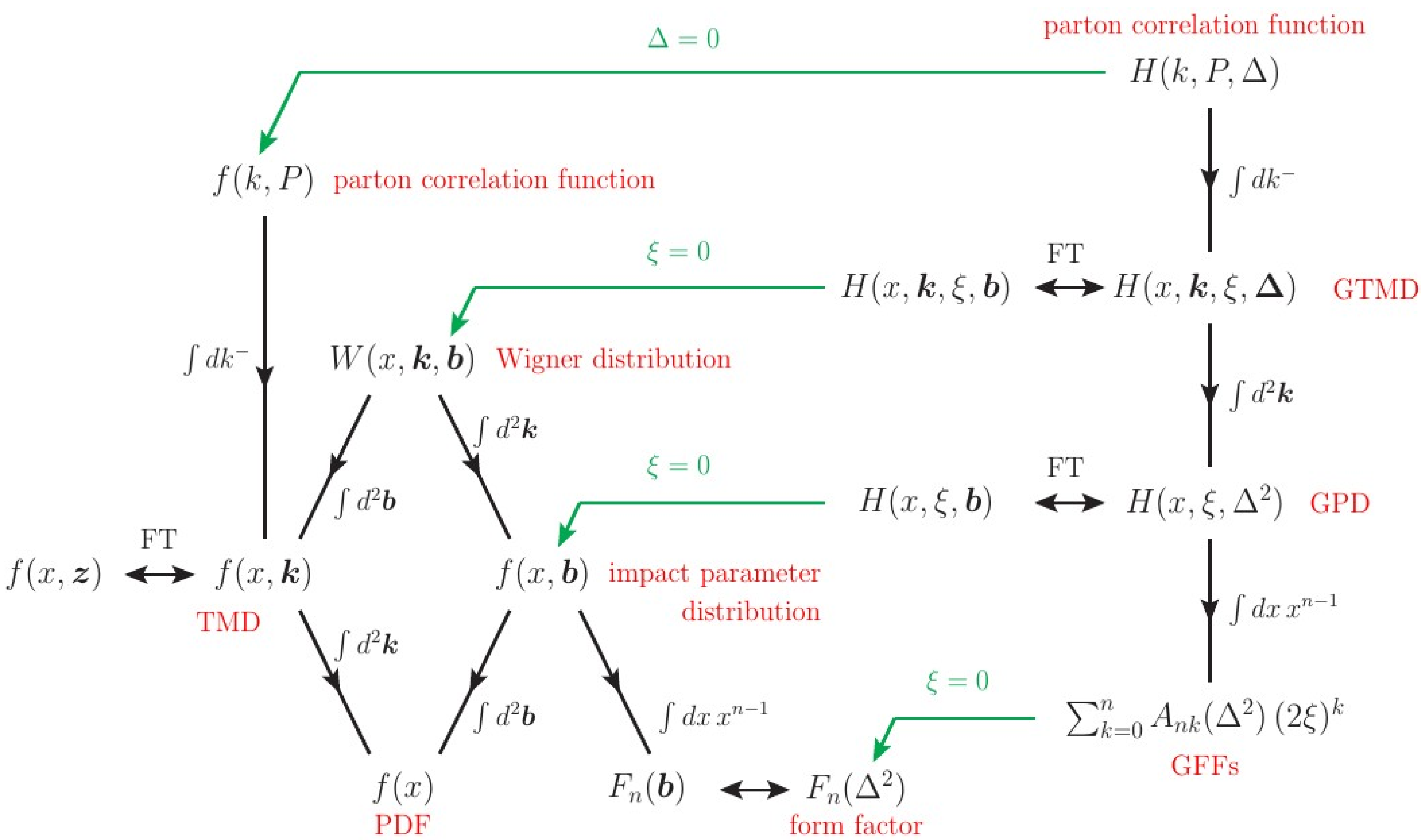

GPCF/GTMD/GPD

GPCFs

$$W^{\Gamma}_{\Lambda,\Lambda'} = \int \frac{d^4 z}{(2\pi)^4} e^{ik\cdot z} \left\langle P + \frac{\Delta}{2} \middle| \overline{\psi}(-\frac{z}{2}) \Gamma \mathcal{U}(-\frac{z}{2}, \frac{z}{2}) \psi(\frac{z}{2}) \middle| P - \frac{\Delta}{2} \right\rangle$$

$$\int dk^-$$

$$W^{\Gamma}_{\Lambda,\Lambda'} = \int \frac{dz^- d^2 z_\perp}{(2\pi)^3} e^{ik\cdot z} \left\langle P + \frac{\Delta}{2} \middle| \overline{\psi}(-\frac{z}{2}) \Gamma \mathcal{U}(-\frac{z}{2}, \frac{z}{2}) \psi(\frac{z}{2}) \middle| P - \frac{\Delta}{2} \right\rangle \Bigg|_{z^+=0}$$

GTMDs

$$\int d^2 k_\perp$$

$$W^{\Gamma}_{\Lambda,\Lambda'} = \int \frac{dz^-}{2\pi} e^{ixP^+ z^-} \left\langle P + \frac{\Delta}{2} \middle| \overline{\psi}(-\frac{z}{2}) \Gamma \mathcal{U}(-\frac{z}{2}, \frac{z}{2}) \psi(\frac{z}{2}) \middle| P - \frac{\Delta}{2} \right\rangle$$

GPDs

Sum Rules for OAM

No framework yet for GTMD observables

$$\frac{d}{dx}\int d^2k_T\,\frac{k_T^2}{M^2}F_{1,4} = H + E + \widetilde{E}_{2T}$$

Twist-2 **Twist-3**

Can we disentangle the Twist-3 GPDs from data?

Exclusive Imaging

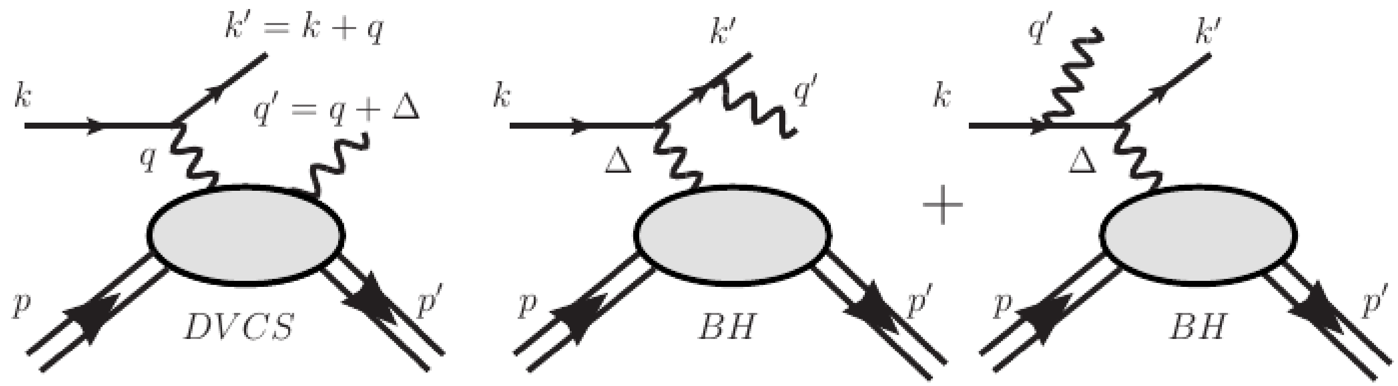

$$|T|^2 = |T_{\rm BH} + T_{\rm DVCS}|^2 = |T_{\rm BH}|^2 + |T_{\rm DVCS}|^2 + \mathcal{I}$$

$$\text{(DVCS)} \quad \gamma^*(q) + p \to \gamma'(q') + p',$$

$$\text{(BH)} \quad \gamma^*(q) + p \to p'$$

$$\mathcal{I} = T^*_{BH} T_{DVCS} + T^*_{DVCS} T_{BH}.$$

DVCS + BH

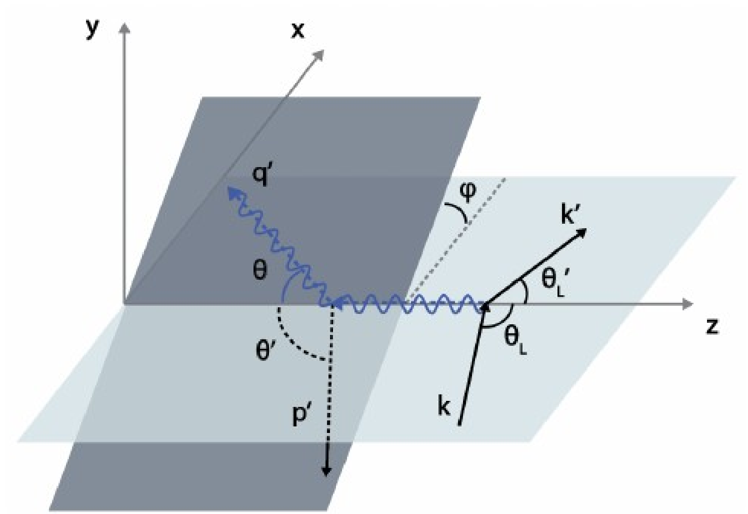

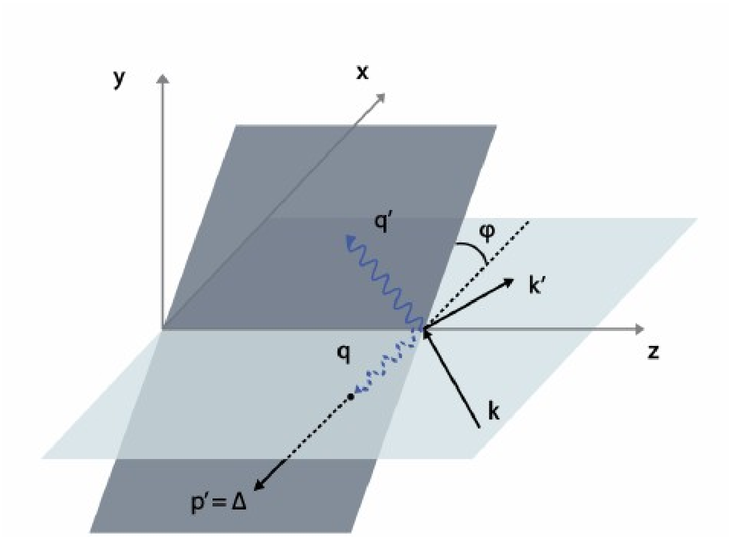

$$|T|^2 = |T_{\rm BH} + T_{\rm DVCS}|^2 = |T_{\rm BH}|^2 + |T_{\rm DVCS}|^2 + \mathcal{I}$$

$$(\text{DVCS}) \quad \gamma^*(q) + p \to \gamma'(q') + p',$$
$$(\text{BH}) \quad \gamma^*(q) + p \to p'$$

$$\mathcal{I} = T^*_{BH} T_{DVCS} + T^*_{DVCS} T_{BH}.$$

Standard School

Dieter Müller

$$|\mathcal{T}_{\rm BH}|^2 = \frac{e^6(1+\epsilon^2)^{-2}}{x_{\rm Bj}^2 y^2 \Delta^2 \mathcal{P}_1(\phi)\mathcal{P}_2(\phi)} \left\{ c_0^{\rm BH} + \sum_{n=1}^{2} c_n^{\rm BH} \cos(n\phi) \right\},$$

exactly known (LO, QED)

$$|\mathcal{T}_{\rm DVCS}|^2 = \frac{e^6}{y^2 \mathcal{Q}^2} \left\{ c_0^{\rm DVCS} + \sum_{n=1}^{2} \left[c_n^{\rm DVCS} \cos(n\phi) + s_n^{\rm DVCS} \sin(n\phi) \right] \right\},$$

harmonics ⇕ 1:1 helicity ampl.

$$\mathcal{I} = \frac{\pm e^6}{x_{\rm Bj} y^3 \Delta^2 \mathcal{P}_1(\phi)\mathcal{P}_2(\phi)} \left\{ c_0^{\mathcal{I}} + \sum_{n=1}^{3} \left[c_n^{\mathcal{I}} \cos(n\phi) + s_n^{\mathcal{I}} \sin(n\phi) \right] \right\}.$$

harmonics ⇕ 1:1 helicity ampl.

chiral even GPDs: $F = \{H, E, \widetilde{H}, \widetilde{E}\}$ *& CFFs:* $\mathcal{F} = \{\mathcal{H}, \mathcal{E}, \widetilde{\mathcal{H}}, \widetilde{\mathcal{E}}\}$

chiral odd GPDs: $F_T = \{H_T, E_T, \widetilde{H}_T, \widetilde{E}_T\}$ $\mathcal{F}_T = \{\mathcal{H}_T, \mathcal{E}_T, \widetilde{\mathcal{H}}_T, \widetilde{\mathcal{E}}_T\}$

DCVS Cross Section: Azimuthal Analysis

$Q^2 = 2.36$ GeV^2, $x_B = 0.37$, $-t = 0.32$ GeV^2

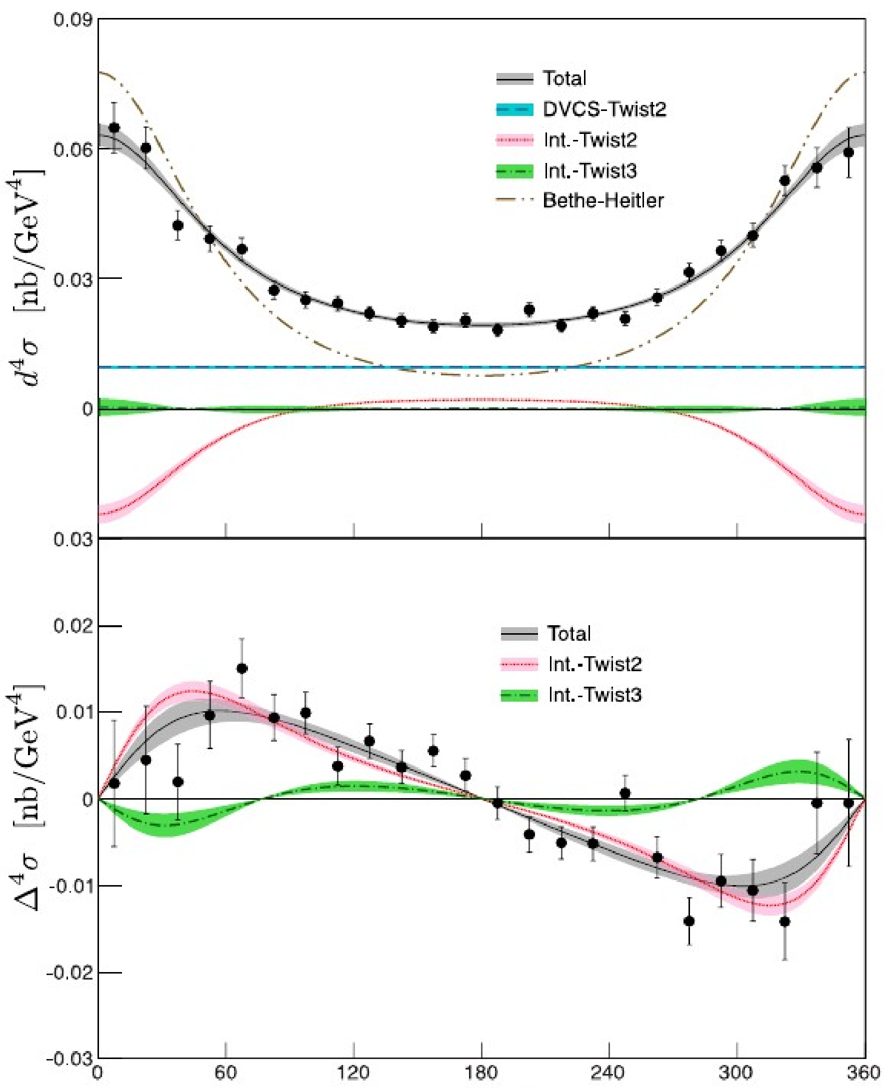

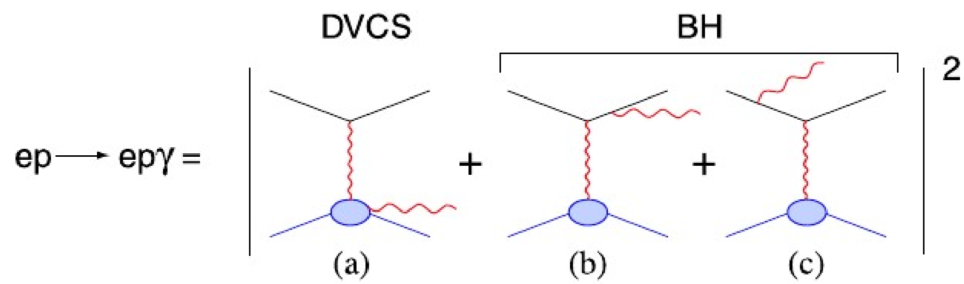

$$d^4\sigma = \mathcal{T}_{\mathrm{BH}}^2 + \mathcal{T}_{\mathrm{BH}}\mathcal{R}e(\mathcal{T}_{\mathrm{DVCS}}) + \mathcal{T}_{\mathrm{DVCS}}^2$$

$$\mathcal{R}e(\mathcal{T}_{\mathrm{DVCS}}) \sim c_0^{\mathcal{I}} + c_1^{\mathcal{I}}\cos\phi + c_2^{\mathcal{I}}\cos 2\phi$$

$$\mathcal{T}_{\mathrm{DVCS}}^2 \sim c_0^{\mathrm{DVCS}} + c_1^{\mathrm{DVCS}}\cos\phi$$

$$\Delta^4\sigma = \frac{d^4\overrightarrow{\sigma} - d^4\overleftarrow{\sigma}}{2} = \mathcal{I}m(\mathcal{T}_{\mathrm{DVCS}})$$

$$\mathcal{I}m(\mathcal{T}_{\mathrm{DVCS}}) \sim s_1^{\mathcal{I}}\sin\phi + s_2^{\mathcal{I}}\sin 2\phi$$

M. Defurne *et al.* Phys. Rev. C 92, 055202

Measuring DVCS

- Helpful Observables
  - Absolute cross section
  - Spin Asymmetries
  - Charge asymmetries
- Extraction of CFFs
  - A complete set of measurements possible
- So far only Hermes

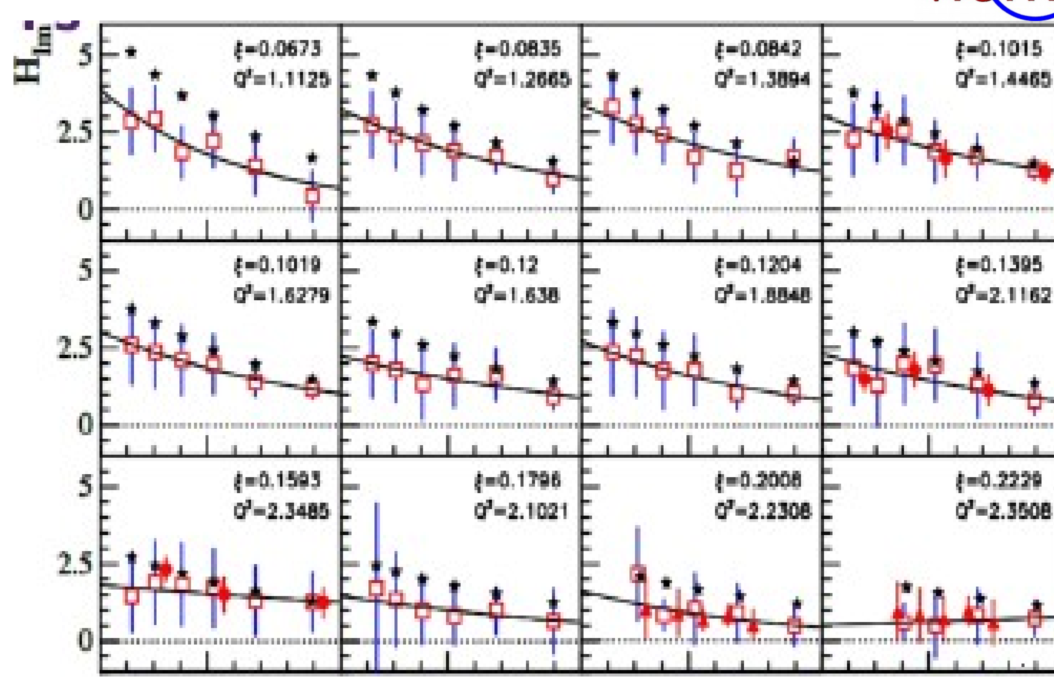

Proton Tomography

- CFFs are directly linked to the tomography of the proton

  - The mean squared charge radius of the proton for slices of x

  - Error bars reflect a factor 5 of the model for unconstrained CFFs

- Nucleon size shrinking with x

  - Proof of framework?

- New observables needed

  - Critical for spin structure

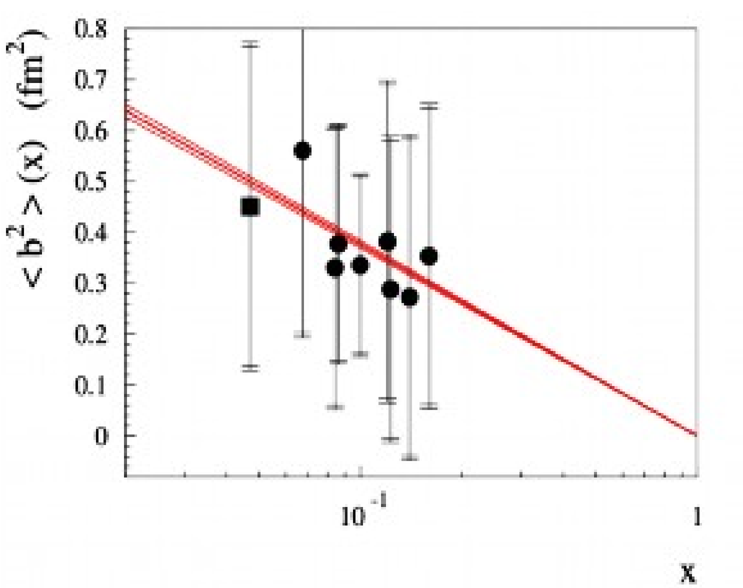

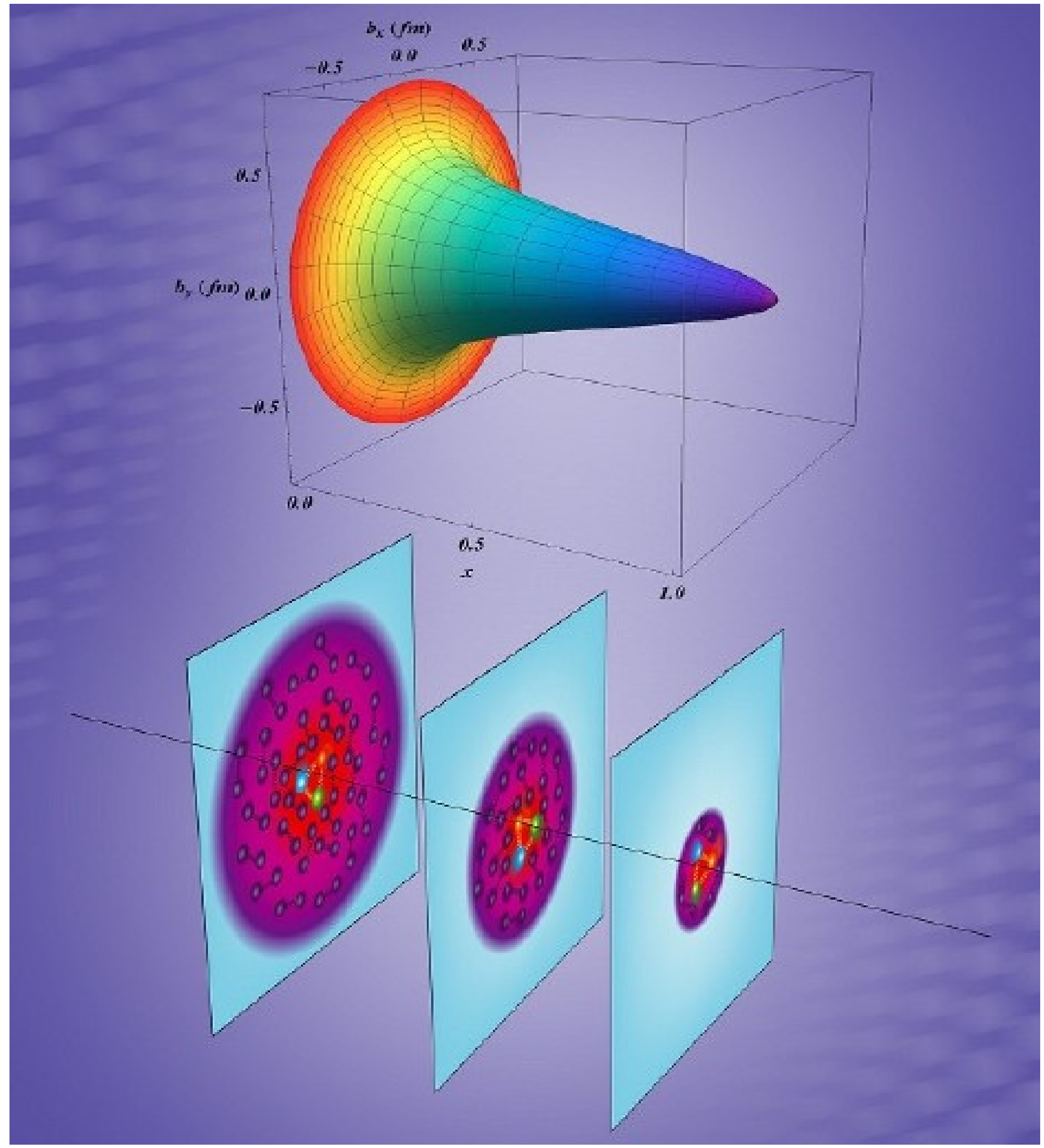

DVCS Cross Section

$$\frac{d^5\sigma_{DVCS}}{dx_{Bj}dQ^2d|t|d\phi d\phi_S} = \Gamma\left|T_{DVCS}\right|^2$$

Unpolarized →
$$= \frac{\Gamma}{Q^2(1-\epsilon)}\Big\{F_{UU,T} + \epsilon F_{UU,L} + \epsilon\cos 2\phi F_{UU}^{\cos 2\phi} + \sqrt{\epsilon(\epsilon+1)}\cos\phi F_{UU}^{\cos\phi}$$

LU polarized →
$$+ (2h)\sqrt{2\epsilon(1-\epsilon)}\sin\phi F_{LU}^{\sin\phi}$$

UL polarized →
$$+ (2\Lambda)\Big[\sqrt{\epsilon(\epsilon+1)}\sin\phi F_{UL}^{\sin\phi} + \epsilon\sin 2\phi F_{UL}^{\sin 2\phi}$$

LL polarized →
$$+ (2h)\left(\sqrt{1-\epsilon^2}F_{LL} + 2\sqrt{\epsilon(1-\epsilon)}\cos\phi F_{LL}^{\cos\phi}\right)\Big]$$

UT polarized →
$$+ (2\Lambda_T)\Big[\sin(\phi-\phi_S)\left(F_{UT,T}^{\sin(\phi-\phi_S)} + \epsilon F_{UT,L}^{\sin(\phi-\phi_S)}\right)$$
$$+ \quad \epsilon\sin(\phi+\phi_S)F_{UT}^{\sin(\phi+\phi_S)} + \epsilon\sin(3\phi-\phi_S)F_{UT}^{\sin(3\phi-\phi_S)}$$
$$+\sqrt{2\epsilon(1+\epsilon)}\left(\sin\phi_S F_{UT}^{\sin\phi_S} + \sin(2\phi-\phi_S)F_{UT}^{\sin(2\phi-\phi_S)}\right)\Big]$$

LT polarized →
$$+(2h)(2\Lambda_T)\Big[\sqrt{1-\epsilon^2}\cos(\phi-\phi_S)F_{LT}^{\cos(\phi-\phi_S)} + \sqrt{2\epsilon(1-\epsilon)}\cos\phi_S F_{LT}^{\cos\phi_S}$$
$$+\sqrt{2\epsilon(1-\epsilon)}\cos(2\phi-\phi_S)F_{LT}^{\cos(2\phi-\phi_S)}\Big]\Big\}$$

- Twist 2: $F_{UU,T}$, F_{LL}, $F_{UT,T}^{\sin(\phi-\phi_S)}$, $F_{LT}^{\cos(\phi-\phi_S)}$
- Twist 3: $F_{UU}^{\cos\phi}$, $F_{UL}^{\sin\phi}$, $F_{LU}^{\sin\phi}$, $F_{LL}^{\cos\phi}$, $F_{UT}^{\sin\phi_S}$, $F_{UT}^{\sin(2\phi-\phi_S)}$, $F_{LT}^{\cos\phi_S}$, $F_{LT}^{\cos(2\phi-\phi_S)}$
- Twist 4: $F_{UU,L}$, $F_{UT,L}^{\sin(\phi-\phi_s)}$

DVCS

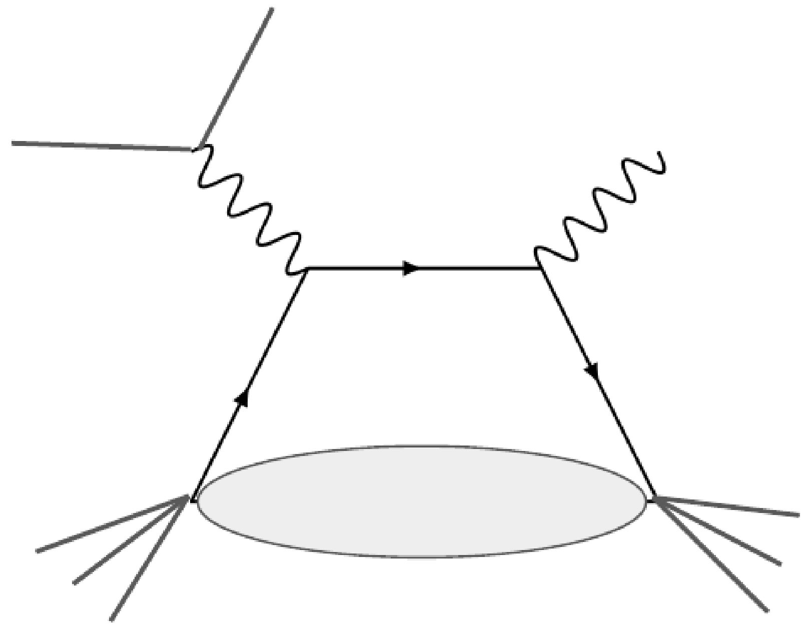

Twist - 2

Twist - 3

$$W^{\mu\nu} \propto \gamma^\mu \gamma^+ \gamma^\nu = \begin{bmatrix} \gamma^- & \gamma^1 - i\gamma^2\gamma_5 & \gamma^2 + i\gamma^1\gamma_5 & i\gamma^-\gamma_5 \\ \gamma^1 + i\gamma^2\gamma_5 & \gamma^+ & i\gamma^+\gamma_5 & -\gamma^1 - i\gamma^2\gamma_5 \\ \gamma^2 - i\gamma^1\gamma_5 & -i\gamma^+\gamma_5 & \gamma^+ & -\gamma^2 + i\gamma^1\gamma_5 \\ -i\gamma^-\gamma_5 & -\gamma^1 + i\gamma^2\gamma_5 & -\gamma^2 - i\gamma^1\gamma_5 & \gamma^- \end{bmatrix}$$

Twist-2 Observables

$$F_{UU,T} = 4\Big[(1-\xi^2)\left(|\mathcal{H}|^2 + |\tilde{\mathcal{H}}|^2\right) + \frac{t_o - t}{2M^2}\left(|\mathcal{E}|^2 + \xi^2 |\tilde{\mathcal{E}}|^2\right) - \frac{2\xi^2}{1-\xi^2}\,\Re\mathrm{e}\left(\mathcal{H}\mathcal{E} + \widetilde{\mathcal{H}}\widetilde{\mathcal{E}}\right)\Big]$$

$$F_{LL} = 2\left[2(1-\xi^2)\ |\mathcal{H}\widetilde{\mathcal{H}}| + 4\xi\,\frac{t_o - t}{2M^2}\ |\mathcal{E}\widetilde{\mathcal{E}}| + \frac{2\xi^2}{1-\xi^2}\Re\mathrm{e}\left(\mathcal{H}\widetilde{\mathcal{E}} + \widetilde{\mathcal{H}}\mathcal{E}\right)\right]$$

$$F_{UT,T}^{\sin(\phi-\phi_S)} = -\frac{\sqrt{t_0 - t}}{2M}\Big[\Re e\left(\widetilde{\mathcal{H}} - \tfrac{\xi^2}{1-\xi^2}\widetilde{\mathcal{E}}\right)\Im m\mathcal{E} - \xi\,\Re e\left(\mathcal{H} - \tfrac{\xi^2}{1-\xi^2}\mathcal{E}\right)\Im m\widetilde{\mathcal{E}}$$

$$- \Im m\left(\widetilde{\mathcal{H}} - \tfrac{\xi^2}{1-\xi^2}\widetilde{\mathcal{E}}\right)\Re e\mathcal{E} + \xi\,\Im m\left(\mathcal{H} - \tfrac{\xi^2}{1-\xi^2}\mathcal{E}\right)\Re e\widetilde{\mathcal{E}}\Big]$$

Twist-3 Observables

$$F_{UU}^{\cos\phi} = -2\,(1-\xi^2)\Re\mathrm{e}\Big[\Big(2\widetilde{\mathcal{H}}_{2T} + \mathcal{E}_{2T} + 2\widetilde{\mathcal{H}}'_{2T} + \mathcal{E}'_{2T}\Big)\Big(\mathcal{H} - \frac{\xi^2}{1-\xi^2}\mathcal{E}\Big) - 2\xi\Big(\widetilde{\mathcal{E}}_{2T} + \widetilde{\mathcal{E}}'_{2T}\Big)\Big(\widetilde{\mathcal{H}} - \frac{\xi^2}{1-\xi^2}\widetilde{\mathcal{E}}\Big) + \frac{t_0-t}{16M^2}\Big(\widetilde{\mathcal{H}}_{2T} + \widetilde{\mathcal{H}}'_{2T}\Big)\Big(\mathcal{E} + \xi\widetilde{\mathcal{E}}\Big) + \Big(\mathcal{H}_{2T} + \mathcal{H}'_{2T} + \frac{t_0-t}{4M^2}\Big(\widetilde{\mathcal{H}}_{2T} + \widetilde{\mathcal{H}}'_{2T}\Big) + \frac{\xi}{1-\xi^2}\Big(\widetilde{\mathcal{E}}_{2T} + \widetilde{\mathcal{E}}'_{2T}\Big) - \frac{\xi^2}{1-\xi^2}\Big(\mathcal{E}_{2T} + \mathcal{E}'_{2T}\Big)\Big)\Big(\mathcal{E} - \xi\widetilde{\mathcal{E}}\Big)\Big]$$

What are these linear combinations of GPDs?

$$F_{LU}^{\sin\phi} = -2\,(1-\xi^2)\Im\mathrm{m}\Big[\Big(2\widetilde{\mathcal{H}}_{2T} + \mathcal{E}_{2T} + 2\widetilde{\mathcal{H}}'_{2T} + \mathcal{E}'_{2T}\Big)\Big(\mathcal{H} - \frac{\xi^2}{1-\xi^2}\mathcal{E}\Big) - 2\xi\Big(\widetilde{\mathcal{E}}_{2T} + \widetilde{\mathcal{E}}'_{2T}\Big)\Big(\widetilde{\mathcal{H}} - \frac{\xi^2}{1-\xi^2}\widetilde{\mathcal{E}}\Big) + \frac{t_0-t}{16M^2}\Big(\widetilde{\mathcal{H}}_{2T} + \widetilde{\mathcal{H}}'_{2T}\Big)\Big(\mathcal{E} + \xi\widetilde{\mathcal{E}}\Big) + \Big[\Big(\mathcal{H}_{2T} + \mathcal{H}'_{2T} + \frac{t_0-t}{4M^2}\Big(\widetilde{\mathcal{H}}_{2T} + \widetilde{\mathcal{H}}'_{2T}\Big) + \frac{\xi}{1-\xi^2}\Big(\widetilde{\mathcal{E}}_{2T} + \widetilde{\mathcal{E}}'_{2T}\Big) - \frac{\xi^2}{1-\xi^2}\Big(\mathcal{E}_{2T} + \mathcal{E}'_{2T}\Big)\Big)\Big(\mathcal{E} - \xi\widetilde{\mathcal{E}}\Big)\Big]$$

Get access to 8 Form Factors from DVCS alone.

Observables

GPD	Twist	$P_q P_p$	TMD
$\mathbf{H} + \frac{\xi^2}{1-\xi} E$	2	UU	f_1
$\widetilde{\mathbf{H}} + \frac{\xi^2}{1-\xi} \widetilde{E}$	2	LL	g_1
$\mathbf{E}$	2	UT	$f_{1T}^{\perp\,(*)}$
$\widetilde{\mathbf{E}}$	2	LT	g_{1T}
$\mathbf{H+E}$	2	-	-

GPD	Twist	$P_q P_p$	TMD
$\mathbf{2\widetilde{H}_{2T} + E_{2T}} - \xi \widetilde{E}_{2T}$	3	UU	$f^{\perp}$
$\mathbf{2\widetilde{H}'_{2T} + E'_{2T}} - \xi \widetilde{E}'_{2T}$	3	LL	$g_L^{\perp}$
$\mathbf{H_{2T}} + \frac{\mathbf{t_o - t}}{\mathbf{4M^2}} \mathbf{\widetilde{H}_{2T}}$	3	UT	$f_T^{(*)}, f_T^{\perp\,(*)}$
$\mathbf{H'_{2T}} + \frac{\mathbf{t_o - t}}{\mathbf{4M^2}} \mathbf{\widetilde{H}'_{2T}}$	3	LT	$g'_T, g_T^{\perp}$
$\mathbf{\widetilde{E}_{2T}} - \xi E_{2T}$	3	UL	$f_L^{\perp\,(*)}$
$\mathbf{\widetilde{E}'_{2T}} - \xi E'_{2T}$	3	LU	$g^{\perp\,(*)}$
$\mathbf{\widetilde{H}_{2T}}$	3	UT_x	$f_T^{\perp\,(*)}$
$\mathbf{\widetilde{H}'_{2T}}$	3	LT_x	$g_T^{\perp}$

Additional Information

OAM $$\frac{1}{\sqrt{1-\xi^2}}\frac{\Delta_\perp}{P^+}\left(\widetilde{E}_{2T} - \xi E_{2T}\right)e^{i\phi} = W^{\gamma^1}_{++} + iW^{\gamma^2}_{++} - W^{\gamma^1}_{--} - iW^{\gamma^2}_{--}$$

$$\frac{1}{\sqrt{1-\xi^2}}\frac{\Delta_\perp}{P^+}\left(E_{2T} - \xi \widetilde{E}_{2T} + 2\widetilde{H}_{2T}\right)e^{i\phi} = W^{\gamma^1}_{++} + iW^{\gamma^2}_{++} + W^{\gamma^1}_{--} + iW^{\gamma^2}_{--}$$

$$\frac{1}{\sqrt{1-\xi^2}}\frac{\Delta_\perp^2}{MP^+}2\widetilde{H}_{2T} = \left(W^{\gamma^1}_{-+} - iW^{\gamma^2}_{-+}\right)e^{2i\phi} - \left(W^{\gamma^1}_{+-} + iW^{\gamma^2}_{+-}\right)e^{-2i\phi}$$

$$\frac{1}{\sqrt{1-\xi^2}}\frac{4M}{P^+}\left(\widetilde{E}_{2T} - \xi E_{2T} - (1-\xi^2)H_{2T} - \frac{\Delta_\perp^2}{4M^2}\widetilde{H}_{2T}\right) = W^{\gamma^1}_{+-} - iW^{\gamma^2}_{+-} - W^{\gamma^1}_{-+} - iW^{\gamma^2}_{-+}$$

Additional Information

$$\frac{1}{\sqrt{1-\xi^2}}\frac{\Delta_\perp}{P^+}\left(\widetilde{E}'_{2T} - \xi E'_{2T}\right)e^{i\phi} = W_{++}^{\gamma^1\gamma_5} + iW_{++}^{\gamma^2\gamma_5} - W_{--}^{\gamma^1\gamma_5} - iW_{--}^{\gamma^2\gamma_5}$$

Spin-Orbit

$$\frac{1}{\sqrt{1-\xi^2}}\frac{\Delta_\perp}{P^+}\left(E'_{2T} - \xi \widetilde{E}'_{2T} + 2\widetilde{H}'_{2T}\right)e^{i\phi} = W_{++}^{\gamma^1\gamma_5} + iW_{++}^{\gamma^2\gamma_5} + W_{--}^{\gamma^1\gamma_5} + iW_{--}^{\gamma^2\gamma_5}$$

$$-\frac{1}{\sqrt{1-\xi^2}}\frac{\Delta_\perp^2}{MP^+}2\widetilde{H}'_{2T} = \left(W_{+-}^{\gamma^1\gamma_5} + iW_{+-}^{\gamma^2\gamma_5}\right)e^{-2i\phi} + \left(W_{-+}^{\gamma^1\gamma_5} - iW_{-+}^{\gamma^2\gamma^5}\right)e^{2i\phi}$$

$$\frac{1}{\sqrt{1-\xi^2}}\frac{4M}{P^+}\left(\widetilde{E}'_{2T} - \xi E'_{2T} + (1-\xi^2)H'_{2T} + \frac{\Delta_T^2}{4M^2}\widetilde{H}'_{2T}\right) = W_{+-}^{\gamma^1\gamma_5} - iW_{+-}^{\gamma^2\gamma_5} + W_{-+}^{\gamma^1\gamma_5} + iW_{-+}^{\gamma^2\gamma_5}$$

Timelike-Spacelike

- Spacelike DIS and timelike Drell-Yan processes both factorize into partonic cross section and a Parton Distribution Function (PDF)
  - Measurement of both demonstrated the universality of PDFs

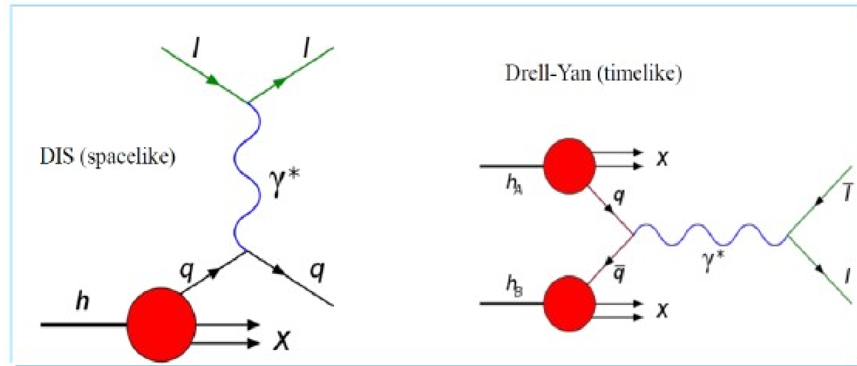

- In Deeply Virtual Compton Scattering (DVCS) there is a similar factorization at the amplitude level into a perturbative coefficient function and a Generalized Parton Distribution (GPD)

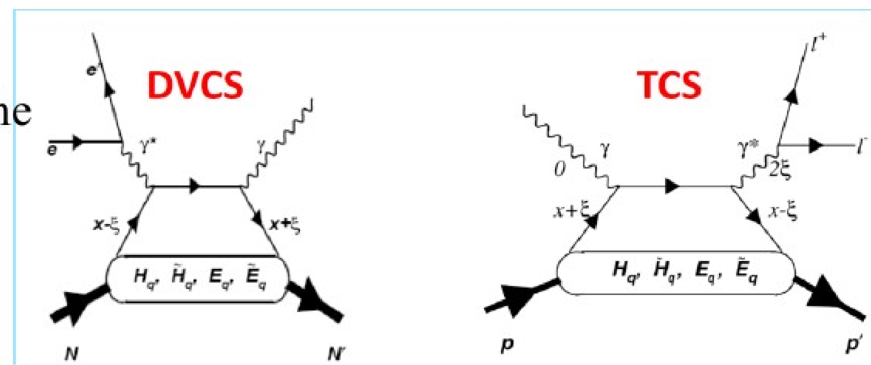

In TCS the real part of the scattering amplitude can be accessed through the azimuthal angular asymmetry of lepton pair (unpolarized beam and target) or through the spin asymmetries (polarized beam and/or polarized target).

Timelike Compton Scattering

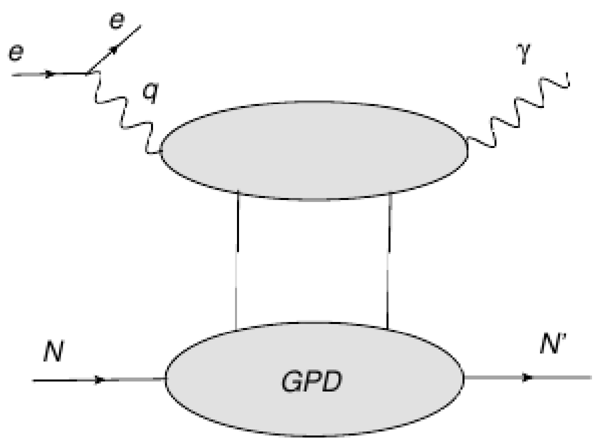

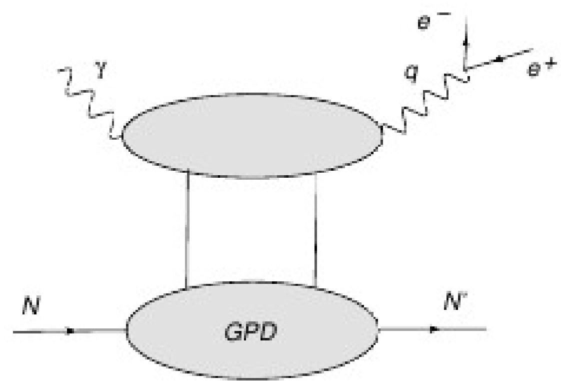

$$\gamma(q)N(p) \rightarrow \gamma^*(q')N(p') \rightarrow l^-(k)l^+(k')N(p')$$

The Time Process

TCS

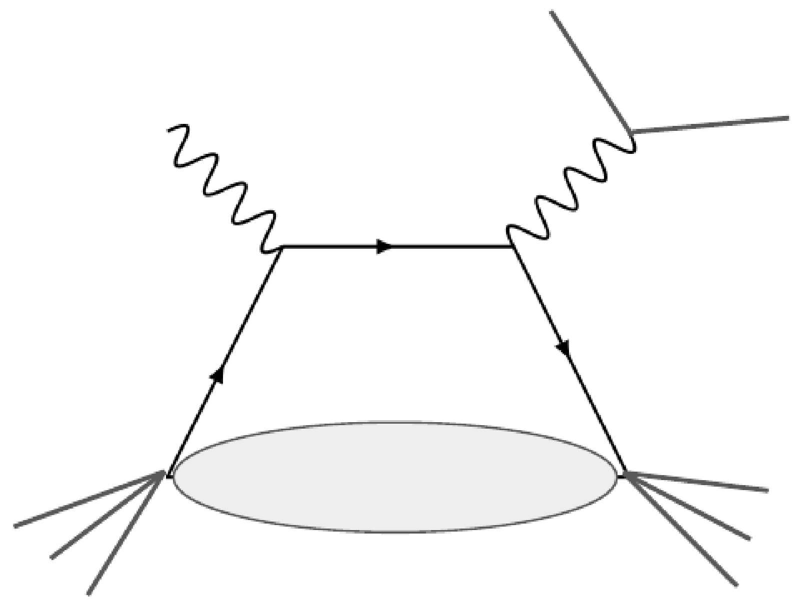

Twist - 2

Twist - 3

$e^{i\phi} \rightarrow e^{-i\phi}$

$$W^{\mu\nu} \propto \gamma^\mu \gamma^+ \gamma^\nu = \begin{bmatrix} \gamma^- & \gamma^1 - i\gamma^2\gamma_5 & \gamma^2 + i\gamma^1\gamma_5 & i\gamma^-\gamma_5 \\ \gamma^1 + i\gamma^2\gamma_5 & \gamma^+ & i\gamma^+\gamma_5 & -\gamma^1 - i\gamma^2\gamma_5 \\ \gamma^2 - i\gamma^1\gamma_5 & -i\gamma^+\gamma_5 & \gamma^+ & -\gamma^2 + i\gamma^1\gamma_5 \\ -i\gamma^-\gamma_5 & -\gamma^1 + i\gamma^2\gamma_5 & -\gamma^2 - i\gamma^1\gamma_5 & \gamma^- \end{bmatrix}$$

Combining Information

TCS

$$F_{UU}^{\cos\phi} = -2\,(1-\xi^2)\Re\mathrm{e}\Big[\Big(2\widetilde{\mathcal{H}}_{2T} + \mathcal{E}_{2T} - 2\widetilde{\mathcal{H}}'_{2T} - \mathcal{E}'_{2T}\Big)\Big(\mathcal{H} - \frac{\xi^2}{1-\xi^2}\mathcal{E}\Big)$$
$$- 2\xi\,\Big(\widetilde{\mathcal{E}}_{2T} - \widetilde{\mathcal{E}}'_{2T}\Big)\Big(\widetilde{\mathcal{H}} - \frac{\xi^2}{1-\xi^2}\widetilde{\mathcal{E}}\Big) + \frac{t_0-t}{16M^2}\Big(\widetilde{\mathcal{H}}_{2T} - \widetilde{\mathcal{H}}'_{2T}\Big)\Big(\mathcal{E} + \xi\widetilde{\mathcal{E}}\Big)$$
$$+ \Big(\mathcal{H}_{2T} - \mathcal{H}'_{2T} + \frac{t_0-t}{4M^2}\Big(\widetilde{\mathcal{H}}_{2T} - \widetilde{\mathcal{H}}'_{2T}\Big) + \frac{\xi}{1-\xi^2}\Big(\widetilde{\mathcal{E}}_{2T} - \widetilde{\mathcal{E}}'_{2T}\Big)$$
$$- \frac{\xi^2}{1-\xi^2}\Big(\mathcal{E}_{2T} - \mathcal{E}'_{2T}\Big)\Big)\Big(\mathcal{E} - \xi\widetilde{\mathcal{E}}\Big)\Big]$$

$$\rightarrow -2\xi\widetilde{\mathcal{E}}_{2T}\widetilde{\mathcal{H}}$$

DVCS

$$F_{UU}^{\cos\phi} = -2\,(1-\xi^2)\Re\mathrm{e}\Big[\Big(2\widetilde{\mathcal{H}}_{2T} + \mathcal{E}_{2T} + 2\widetilde{\mathcal{H}}'_{2T} + \mathcal{E}'_{2T}\Big)\Big(\mathcal{H} - \frac{\xi^2}{1-\xi^2}\mathcal{E}\Big)$$
$$- 2\xi\,\Big(\widetilde{\mathcal{E}}_{2T} + \widetilde{\mathcal{E}}'_{2T}\Big)\Big(\widetilde{\mathcal{H}} - \frac{\xi^2}{1-\xi^2}\widetilde{\mathcal{E}}\Big) + \frac{t_0-t}{16M^2}\Big(\widetilde{\mathcal{H}}_{2T} + \widetilde{\mathcal{H}}'_{2T}\Big)\Big(\mathcal{E} + \xi\widetilde{\mathcal{E}}\Big)$$
$$+ \Big(\mathcal{H}_{2T} + \mathcal{H}'_{2T} + \frac{t_0-t}{4M^2}\Big(\widetilde{\mathcal{H}}_{2T} + \widetilde{\mathcal{H}}'_{2T}\Big) + \frac{\xi}{1-\xi^2}\Big(\widetilde{\mathcal{E}}_{2T} + \widetilde{\mathcal{E}}'_{2T}\Big)$$
$$- \frac{\xi^2}{1-\xi^2}\Big(\mathcal{E}_{2T} + \mathcal{E}'_{2T}\Big)\Big)\Big(\mathcal{E} - \xi\widetilde{\mathcal{E}}\Big)\Big]$$

TCS with HIPS

- Jlab PAC-46: TCS off TPP → E12-18-005

  M. Boer, V. Tadevosyan, DK
- HIPS/CPS: arxiv:1704.00816.pdf B. Wojtsekhowski, D. Day, DK
- NPS: arxiv:1704.00816.pdf, J. Phys. C.S.587012048, arXiv:0609201 T. Horn, R. Ent, NPS Collaboration
- Target/CPS: NIM In Progress DK

Jlab Experimental Setup

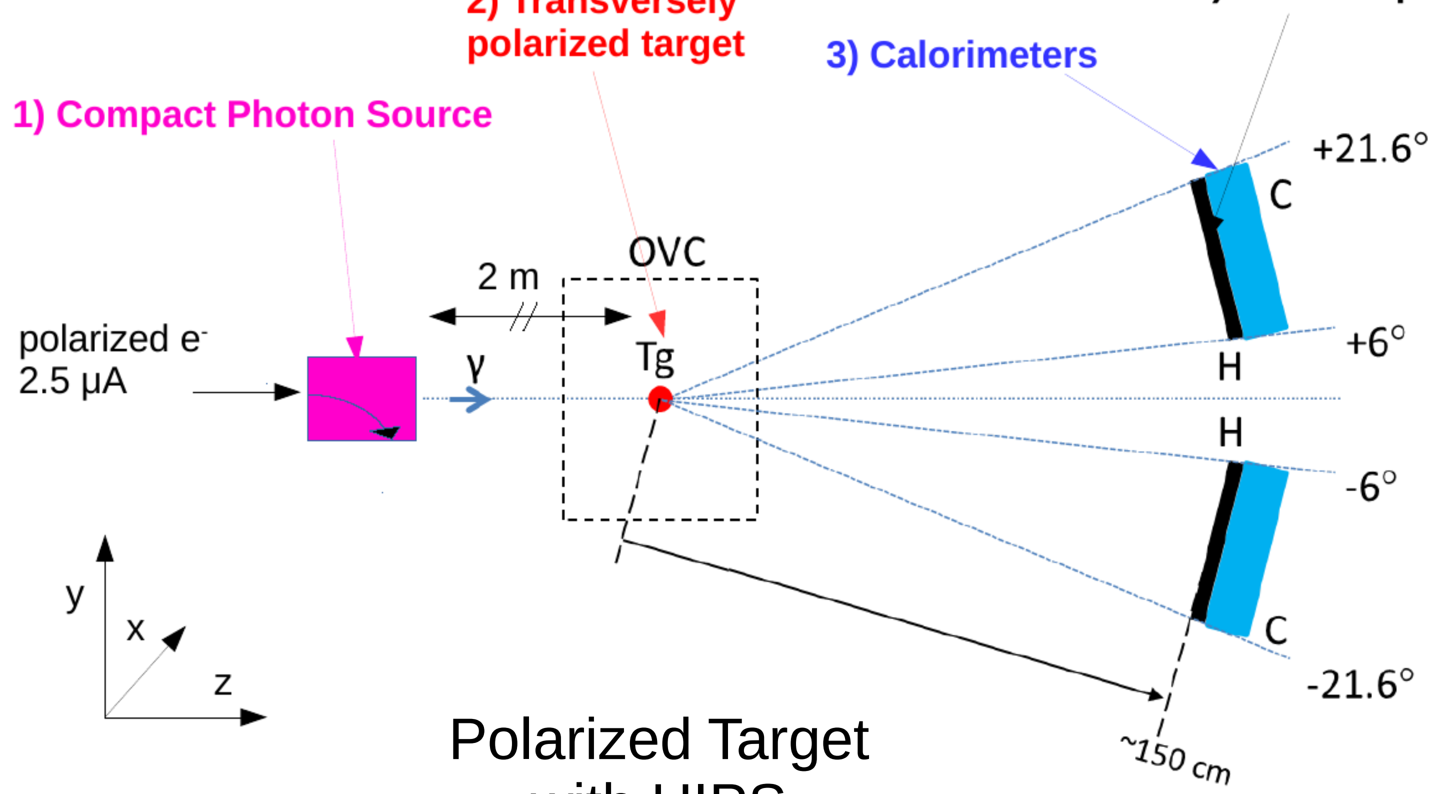

$2.05 \times 2.05 \times 18 cm^3$ $PbWO_4$ crystals

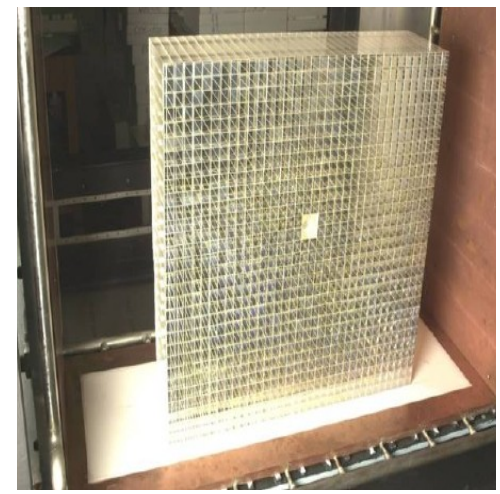

Polarized Target with HIPS

Neutral Particle Spectrometer

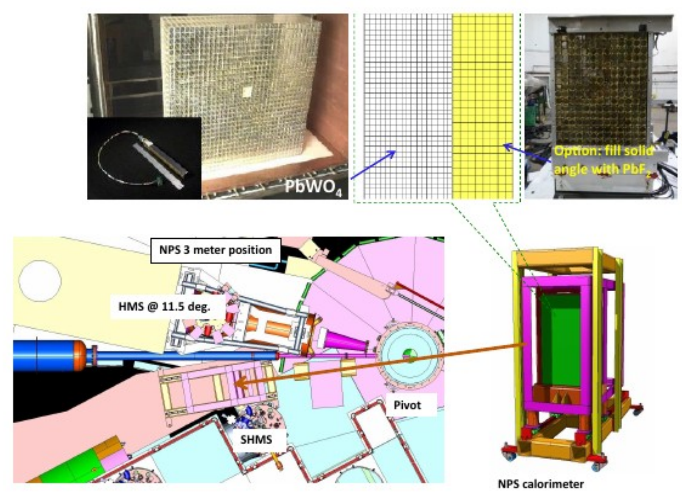

Side view of the TCS experimental setup. Shown are photon beam (γ), transversely polarized target (Tg) in the scattering chamber (OVC), and pairs of hodoscope (H) and calorimeter (C) counters for detection of the recoil proton and the lepton pair.

Compact Photon Source

B. Wojtsekhowski, D. Day, DK

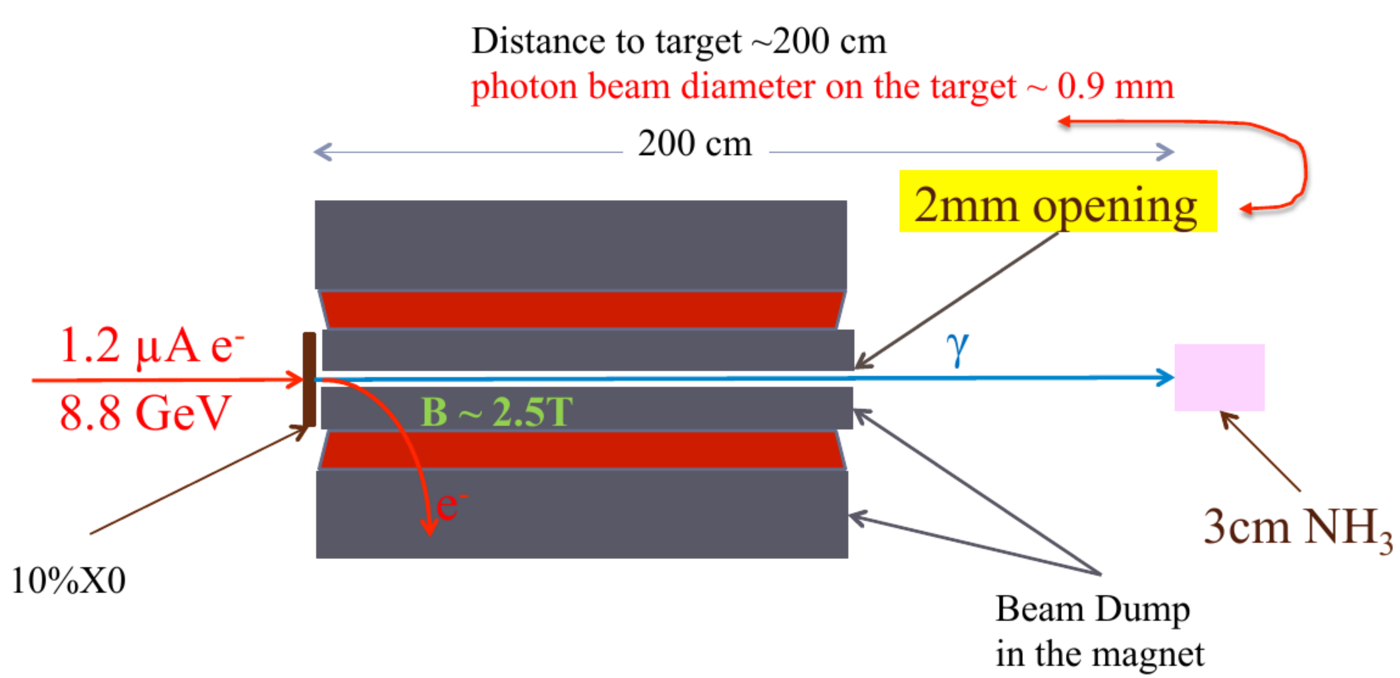

Magnet design

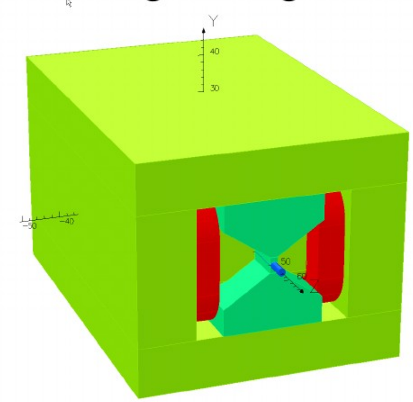

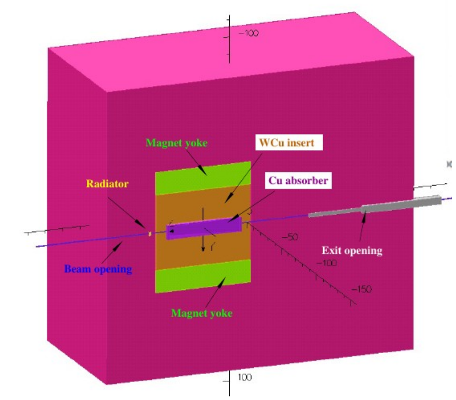

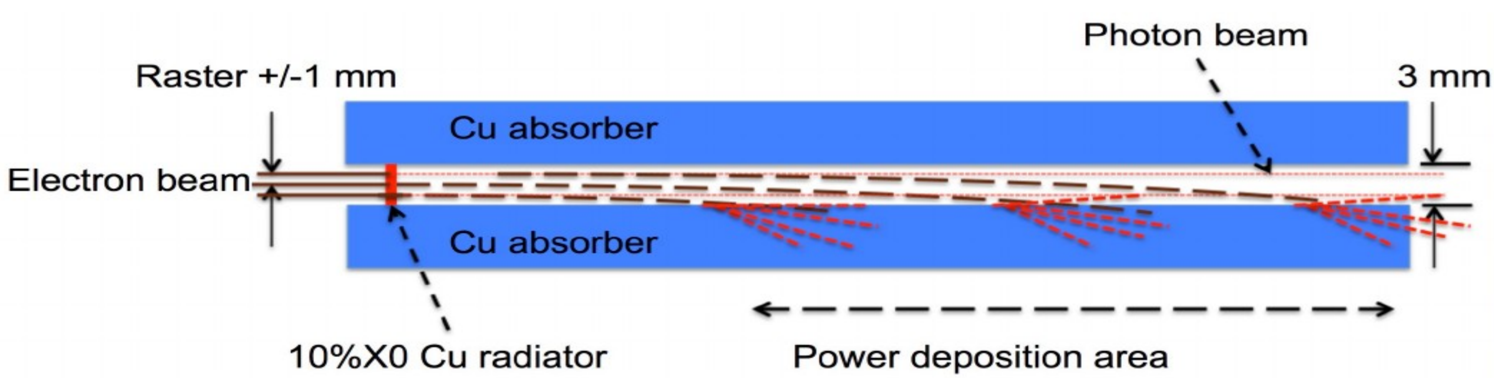

High Intensity Photon Targets

- Depolarization due to radiation damage

  - Photons at the several GeV scale can easily brake up NH3

  - Especially with high energy (IPs) we get significant production of NH2, Atomic H, Atomic N, and recombination to hydrazine and others

  - This radiation damage causes either different polarization mechanisms and/or depleted DNP

  - The production of these free radicals is the leading cause of target maintenance and overhead time required to anneal and replace target material

  - EGS and Geant indicate we will get some of these processes with a high energy photon but the primary production of centers is still NH2, Atomic H from the IPs created by the photon source

  - Secondary scattering of ionizing radiation inside the target using 10^{11} gamma/sec with RMS~1 mm leads to 20 nA of e+/e- in an area of 4.5 mm^2

  - If this dose can be spread out over the surface of the target (570 mm^2) we start to approach the radiation damage seen in CLAS6 type running

- Depolarization due to localized beam heating

  - Local hot-spots caused by interfacial thermal heating can create loss of polarization at the beam location in the target

  - Additional heating issue arise from thermal conductivity of the material and the Kapitza resistance

  - All of this is easily handled by keeping the beam to target position moving (fix only a couple of seconds)

CPS Polarized Target System

- High Intensity High Cooling
- Fixed Photon Beam
- Fixed NMR Sampling
- Manage Beam Heating
- Radiation Damage

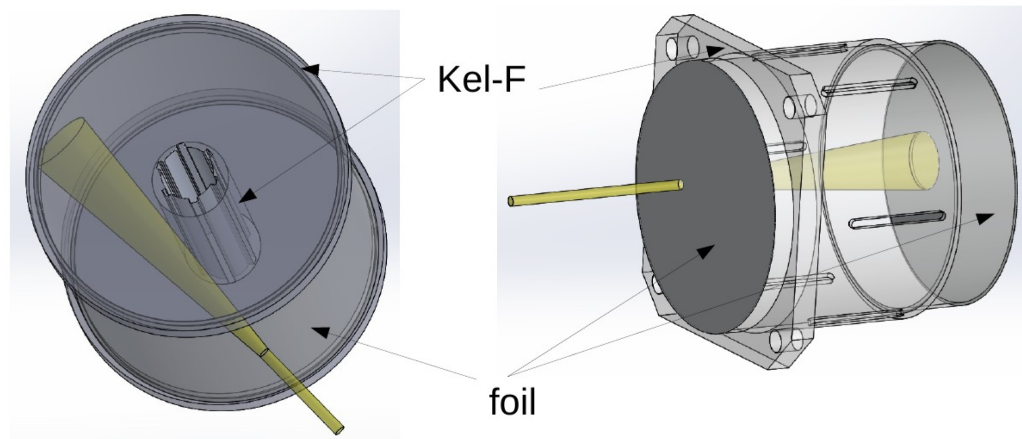

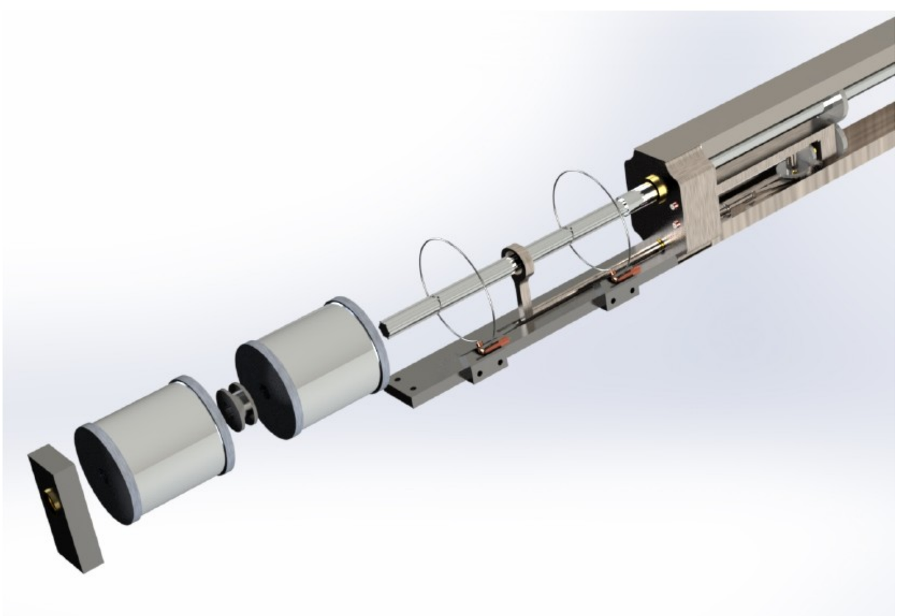

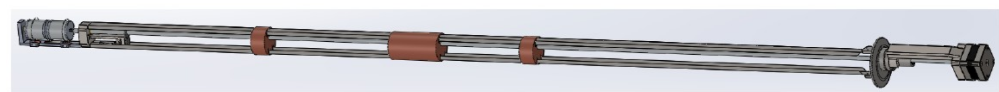

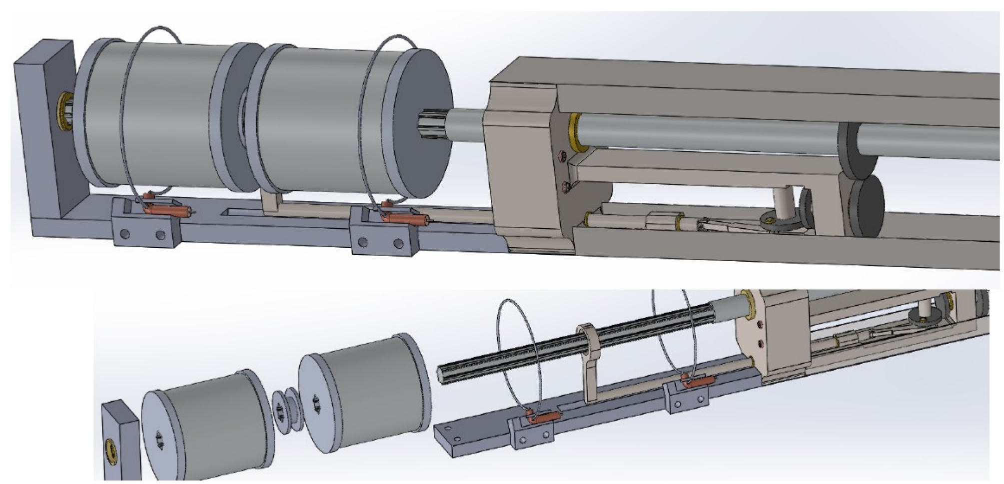

Prospects for Better Experiment

- Higher Energy is Advantageous for TCS

  - BH is smaller

  - Invariant Mass of lepton pair is larger

- Fermilab Photon Beam

  - Primary Production Target

  - Bremsstrahlung

  - Purity/Monochromatic/Intensity/Tagged

Future of Imaging

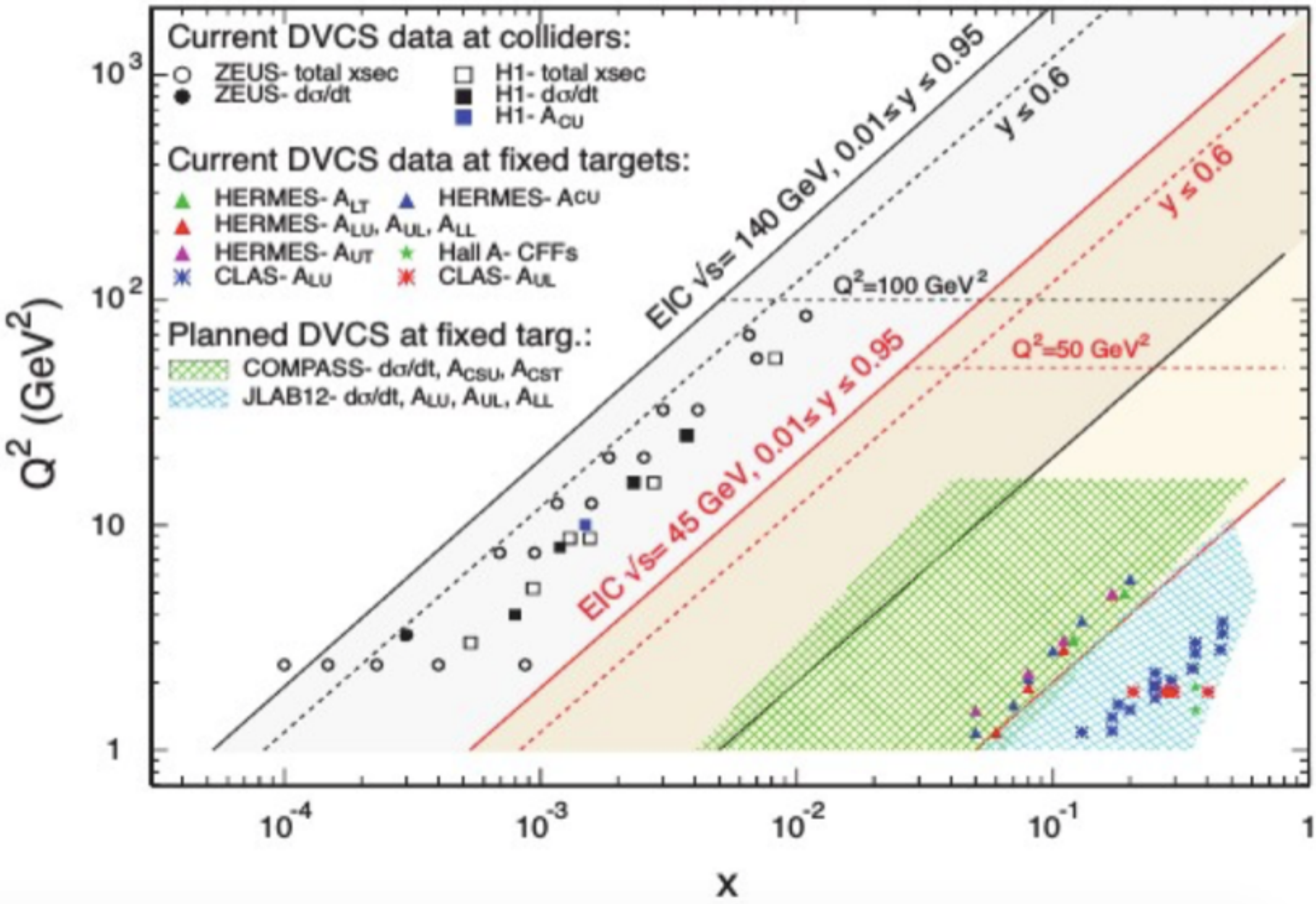

Conclusion

- Get More from the Physics with PT observables
- Tensor Polarized Observables Largely Unexplored (Big Part of Spin Physics)
- Can isolate Twist-3 GPDs of the vector and axial vector sector with T/S-like combination
- Many more fun things to do with PT

Thank You

Take a look

Extraction of Generalized Parton Distribution Observables from Deeply Virtual Electron Proton Scattering Experiments

Brandon Kriesten,[*] Simonetta Liuti,[†] Liliet Calero Diaz,[‡] Dustin Keller,[§] and Andrew Meyer[¶]

Department of Physics, University of Virginia, Charlottesville, VA 22904, USA.

Gary R. Goldstein[**]

Department of Physics and Astronomy, Tufts University, Medford, MA 02155 USA.

J. Osvaldo Gonzalez-Hernandez[††]

INFN, Torino

i) Be General and Covariant
ii) Provide Kinematic Phase Separation
iii) Provide Clear Information Extraction